Article

Neuron

Migrating Interneurons Secrete Fractalkine to Promote Oligodendrocyte Formation in the Developing Mammalian Brain

Highlights

- MGE interneurons promote developmental oligodendrogenesis
- Interneurons secrete paracrine ligands, including fractalkine
- Fractalkine is responsible for interneuron-induced oligodendrocyte genesis
- Fractalkine receptor in precursors is essential for cortical oligodendrogenesis

Authors

Anastassia Voronova, Scott A. Yuzwa, Beatrix S. Wang, ..., Jing Wang, David R. Kaplan, Freda D. Miller

Correspondence

fredam@sickkids.ca

In Brief

Voronova et al. show migrating interneurons act in a paracrine fashion to promote the developmental genesis of oligodendrocytes. They show fractalkine is secreted by interneurons and when fractalkine signaling is inhibited, fewer oligodendrocyte lineage cells are made in the cortex.

Voronova et al., 2017, Neuron *94*, 500–516
May 3, 2017
http://dx.doi.org/10.1016/j.neuron.2017.04.018

CellPress

Neuron
Article

Migrating Interneurons Secrete Fractalkine to Promote Oligodendrocyte Formation in the Developing Mammalian Brain

Anastassia Voronova,[1] Scott A. Yuzwa,[1] Beatrix S. Wang,[1] Siraj Zahr,[1,5] Charvi Syal,[2,3] Jing Wang,[2,3,4] David R. Kaplan,[1,5,6] and Freda D. Miller[1,5,6,7,8,*]
[1]Program in Neurosciences and Mental Health, Hospital for Sick Children, Toronto, ON M5G 1L7, Canada
[2]Regenerative Medicine Program, Ottawa Hospital Research Institute
[3]Department of Cellular and Molecular Medicine
[4]Brain and Mind Research Institute
University of Ottawa, Ottawa, ON K1H 8L6, Canada
[5]Institute of Medical Science
[6]Department of Molecular Genetics
[7]Department of Physiology
University of Toronto, Toronto, ON M5G 1A8, Canada
[8]Lead contact
*Correspondence: fredam@sickkids.ca
http://dx.doi.org/10.1016/j.neuron.2017.04.018

SUMMARY

During development, newborn interneurons migrate throughout the embryonic brain. Here, we provide evidence that these interneurons act in a paracrine fashion to regulate developmental oligodendrocyte formation. Specifically, we show that medial ganglionic eminence (MGE) interneurons secrete factors that promote genesis of oligodendrocytes from glially biased cortical precursors in culture. Moreover, when MGE interneurons are genetically ablated in vivo prior to their migration, this causes a deficit in cortical oligodendrogenesis. Modeling of the interneuron-precursor paracrine interaction using transcriptome data identifies the cytokine fractalkine as responsible for the pro-oligodendrocyte effect in culture. This paracrine interaction is important in vivo, since knockdown of the fractalkine receptor CX3CR1 in embryonic cortical precursors, or constitutive knockout of CX3CR1, causes decreased numbers of oligodendrocyte progenitor cells (OPCs) and oligodendrocytes in the postnatal cortex. Thus, in addition to their role in regulating neuronal excitability, interneurons act in a paracrine fashion to promote the developmental genesis of oligodendrocytes.

INTRODUCTION

Developing mammalian interneurons migrate extensively to populate the CNS. One well-studied example of this process involves interneurons born in the embryonic ganglionic eminences (GE) that migrate into and spread throughout the adjacent cortex (Anderson et al., 1997), where they ultimately regulate levels of neuronal excitability. During their migration, some of these newborn interneurons associate closely with the radial glial precursor cells that generate the excitatory projection neurons and glial cells of the postnatal cortex (Yokota et al., 2007). This close association raises the possibility that migrating interneurons might in some way regulate cortical cell genesis. In this regard, newborn interneurons first arrive in the vicinity of cortical precursors at embryonic day 14, when they are generating neurons (Nadarajah et al., 2002). This association persists throughout late embryonic and early postnatal life, when cortical precursors make virtually all of the astrocytes and oligodendrocytes in the postnatal cortex and white matter tracts (Gauthier-Fisher and Miller, 2013). During this gliogenic period, cortical precursors also make oligodendrocyte precursor cells (OPCs) that persist into adulthood (Kessaris et al., 2006) and, intriguingly, OPCs maintain close interactions with interneurons throughout postnatal development (Orduz et al., 2015).

Here, we have tested the hypothesis that migrating interneurons directly regulate cortical precursor biology. We show that interneurons from the medial GE (MGE) secrete factors that selectively enhance the genesis of oligodendrocytes from glially biased cortical precursors in culture and that when MGE-derived interneurons are genetically ablated in vivo, this causes a deficit in cortical OPCs. Using computational modeling, we define multiple potential paracrine interactions between interneurons and cortical precursors and show that one of the predicted factors, fractalkine, is responsible for the pro-oligodendrogenic effects of MGE interneurons. Finally, we show that knockdown of the fractalkine receptor CX3CR1 in cortical precursors in vivo or the constitutive CX3CR1 knockout causes deficits in OPCs and oligodendrocytes in cortical gray and white matter. Thus, our data indicate that migrating MGE interneurons secrete fractalkine to regulate developmental cortical oligodendrogenesis, and suggest that interneurons might produce fractalkine to regulate OPCs and myelin formation throughout life.

RESULTS

MGE Interneurons Secrete Factors that Instruct Cortical Precursors to Proliferate and Differentiate into Oligodendrocytes in Culture

To ask about potential effects of interneurons on cortical precursors, we first generated purified MGE interneurons by culturing E13 MGE precursor cells for 5 days, during which time they produce many interneurons (Tsui et al., 2014), and adding cytosine arabinoside (AraC) for 24 hr to kill proliferating cells. Immunostaining (Figures 1A and 1B) showed that 90%–95% of cells in these cultures were Gad67-positive, βIII tubulin-positive neurons together with a few GFAP-positive astrocytes and Sox2-positive precursors. No cells expressed the oligodendrocyte marker MBP or the microglial cell marker Iba1.

We generated these purified interneurons from mice carrying a pan-nuclear H2BB-eGFP reporter gene so that they would be genetically tagged, cocultured them with unlabelled E13 cortical precursor cells, and immunostained cultures 2 days later for eGFP to distinguish interneurons, Sox2 to detect precursors, and βIII-tubulin to detect interneurons and newborn cortical excitatory neurons (Figure 1C). Quantification showed that the added interneurons caused an increase in eGFP-negative, Sox2-positive precursors from 57% to 79%, and a coincident decrease in eGFP-negative, βIII-tubulin-positive cortical neurons from 43% to 20% (Figures 1D and 1E). Consistent with this, cortical precursors expressing the proliferation marker Ki67 were increased from 49% to 69% (Figures 1F and 1G). These effects were not due to changes in cell death, since similar low levels of condensed, apoptotic nuclei were observed with and without the added interneurons (Figure 1H).

To ask whether interneurons also affected glial differentiation, we analyzed similar cocultures after 7 days, when glia are first generated (Barnabé-Heider et al., 2005). Immunostainining for GFAP and MBP showed that MGE interneurons increased the genesis of MBP-positive cortical oligodendrocytes, with no effect on GFAP-positive astrocytes (Figures 1I–1K).

To ask whether these changes were due to cell-cell contact versus secreted factors, we performed conditioned medium (CM) experiments. We added fresh medium to MGE interneuron cultures after removing AraC, supplemented the resultant CM with FGF2 and B27 after 2 days, and added it to cultured precursors. Immunostaining 2 days later showed that CM increased Sox2-positive precursors from 56% to 72% and decreased βIII-tubulin-positive neurons from 44% to 28% (Figures 2A–2C). Ki67-positive proliferating precursors were also significantly increased by CM from 46% to 62%, while dying, cleaved caspase 3-positive cells were unaffected (Figures 2D–2F).

We also analyzed gliogenesis at 7 days in culture. Immunostaining demonstrated that MGE interneuron CM increased MBP-positive oligodendrocytes by about 3-fold (Figures 2G and 2H) but had no effect on GFAP-positive astrocytes (Figure 2I). Thus, MGE interneurons secrete factors that enhance proliferation and oligodendroglial differentiation of cortical precursors.

To better characterize these effects, we performed clonal analysis using the piggyBac (PB) transposon system, which allows permanent genomic incorporation of eGFP into single precursors (Gallagher et al., 2015; Nagy et al., 2011). E13 cortical precursors were transfected with the PB eGFP reporter and the PB transposase under conditions where less than 1% of the precursors are labeled. Analysis of these cultures after 7 days in control medium or MGE interneuron CM demonstrated that CM altered the clone size distribution with a significant increase in large clones (>71 cells) (Figures 2J and 2K).

We also asked about gliogenesis, triple-labeling cultures for eGFP, MBP, and GFAP (Figures 2L and 2M). Interneuron CM had no effect on the number of clones containing GFAP-positive astrocytes or the number of GFAP-positive cells per clone (Figures 2N and 2O). In contrast, it significantly increased clones containing MBP-positive cells, and MBP-positive cell numbers per clone (Figures 2P and 2Q). However, the total number of clones containing glial cells was unchanged by CM since almost all oligodendrocyte-contained clones also contained astrocytes (Figure 2R). Instead, astrocyte-only clones were decreased and clones with both astrocytes and oligodendrocytes were coincidentally increased by interneuron CM (Figure 2S). Thus, factor(s) secreted by MGE interneurons direct glially biased cortical precursors to make oligodendrocytes in addition to astrocytes.

MGE Interneurons Regulate the Genesis of Oligodendrocyte Lineage Cells from Cortical Precursors In Vivo

To ask whether, as suggested by these data, MGE interneurons regulate cortical oligodendrogenesis in vivo, we first confirmed that they were present in the embryonic cortical precursor ventricular and subventricular zones (VZ/SVZ), using mice carrying an Nkx2.1-Cre transgene and a YFP reporter gene with an upstream floxed stop cassette in the Rosa26 locus (called YFP^{stop}). In these mice, all MGE precursor progeny will be YFP positive (Xu et al., 2008). Immunostaining of E15 cortical sections from these mice showed that, as previously reported (Xu et al., 2008), MGE-derived, YFP-positive cells were present in the VZ/SVZ, mingled with Pax6-positive radial precursors (Figure 3A). YFP-positive cells were also in the intermediate zone (IZ) and cortical plate (CP), where many were closely associated with nestin-positive basal radial glial precursor cell processes (Figure 3A). We further characterized the YFP-positive cell phenotypes, since the MGE contributes both interneurons and a small, transient population of oligodendrocyte lineage cells to the cortex (Kessaris et al., 2006). Immunostaining of P0 cortical sections showed that a very small proportion (about 6%–7%) of YFP-positive cortical cells expressed the oligodendrocyte lineage marker Olig2 and that these were outside of the SVZ in the apical half of the cortex (Figure 3B). Moreover, only about 10% of total Olig2-positive cells also expressed YFP. Thus, MGE interneurons, but not MGE-derived oligodendrocyte lineage cells, are present in the cortical precursor zones during late embryogenesis and early postnatal life.

We next asked whether MGE interneurons were important for cortical oligodendrogenesis taking advantage of Nkx2.1-Cre mice crossed to mice carrying an active diphtheria toxin A (DTA) fragment with an upstream floxed stop cassette in the *Rosa26* locus (DTA^{stop} mice). In these mice, Nkx2.1-positive cells and their progeny will die embryonically. We injected mothers from these crosses with BrdU at gestational day 18.5

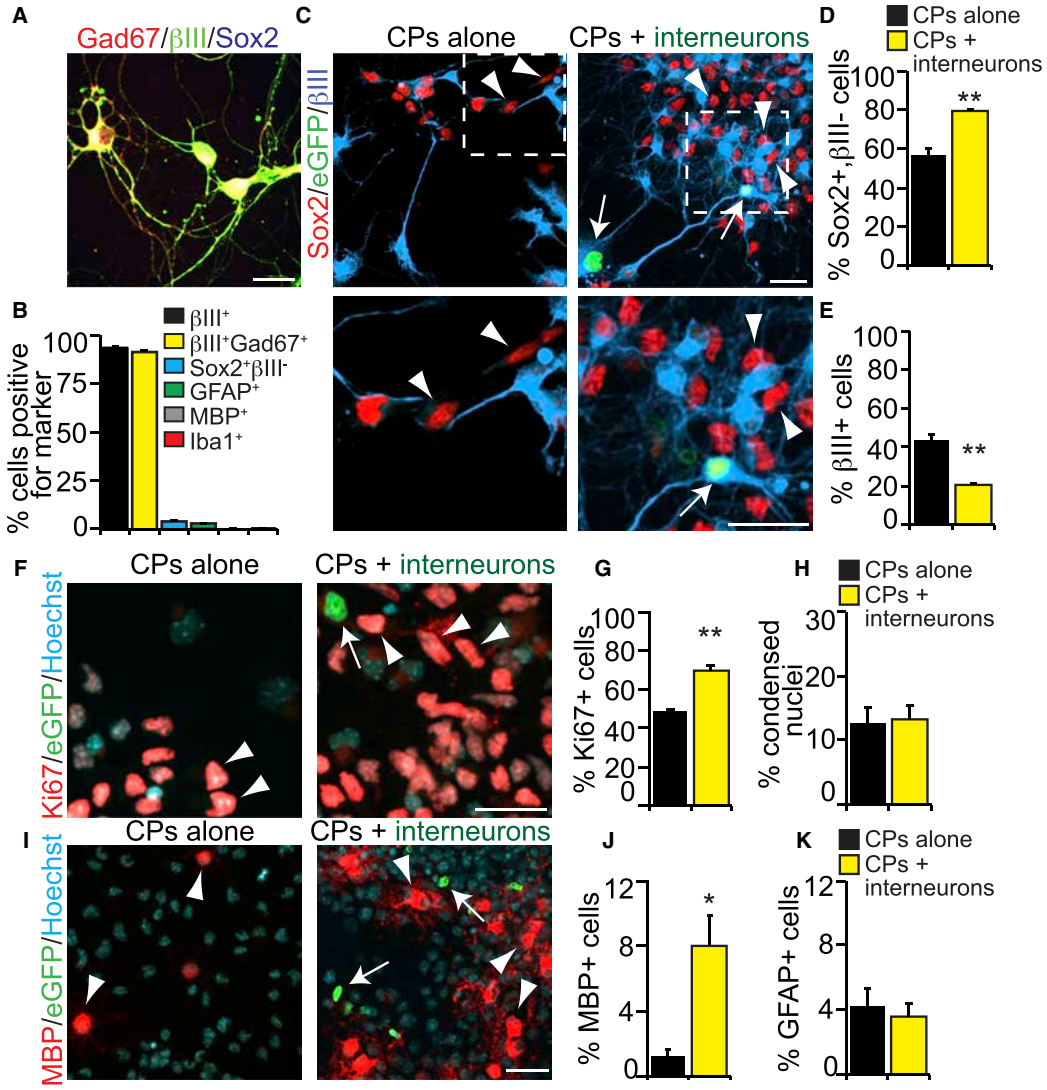

Figure 1. Co-culture of MGE Interneurons with Cortical Precursors Increases Proliferation and Oligodendrogenesis

(A and B) MGE interneurons were generated from E13 MGE precursors, immunostained for Gad67 (red, A), βIII-tubulin (green, A), and Sox2 (blue, A), or for GFAP, MBP, or Iba1, and the percentages of immunopositive cells were determined (B). n = 3 experiments.

(C–K) E13 cortical precursors were cultured alone (CPs alone) or with eGFP-tagged MGE interneurons (CPs + interneurons) for 2 days (C–H) or 7 days (I–K). (C–E) 2 day cultures were immunostained for eGFP (green, C), Sox2 (red, C) and βIII-tubulin (blue, C) and quantified for the percentage of eGFP-negative, βIII-tubulin-negative, Sox2-positive cortical precursors (D, arrowheads in C) or eGFP-negative, βIII-tubulin-positive cortical neurons (E). $^{**}p < 0.01$; n = 3. Arrows in (C) denote eGFP-positive, βIII-tubulin-positive interneurons and hatched boxes are shown at higher magnification in the bottom images. (F and G) Cultures were immunostained for eGFP (green, F) and Ki67 (red, F), counterstained with Hoechst (blue, F), and quantified for the percentage of eGFP-negative, Ki67-positive cortical precursors (G, arrowheads in F). $^{**}p < 0.01$; n = 3. Arrows in (F) denote eGFP-positive interneurons. (H) Quantification of images as in (F) for eGFP-negative cells with condensed nuclei. n = 3 experiments. (I–K) 7 day cultures were immunostained for eGFP (green, I), MBP (red, I) or GFAP, counterstained with Hoechst (blue, I), and quantified for eGFP-negative cells expressing MBP (J, arrowheads in I) or GFAP (K). $^{*}p < 0.05$; $n \geq 3$. Arrows in (I) denote eGFP-positive interneurons. In all graphs, data are expressed as a percentage of total Hoechst-positive cells (B) or Hoechst-positive, eGFP-negative cells (D–K). Scale bars, 20 μm. Error bars represent SEM.

to trace the progeny of embryonic cortical precursors that were dividing at this time point. As controls, we performed similar experiments with mice carrying only the DTA^{stop} transgene, or only the Nkx2.1-Cre transgene. We analyzed these different mice at P0 (Figure S1A), since Nkx2.1-Cre is expressed in non-neural tissues and the Nkx2.1-Cre; DTA^{stop} mice do not survive past birth.

Initially, we confirmed that the ablation strategy worked. Immunostaining identified many somatostatin-positive interneurons in control cortices, with almost none in Nkx2.1-Cre; DTA^{stop}

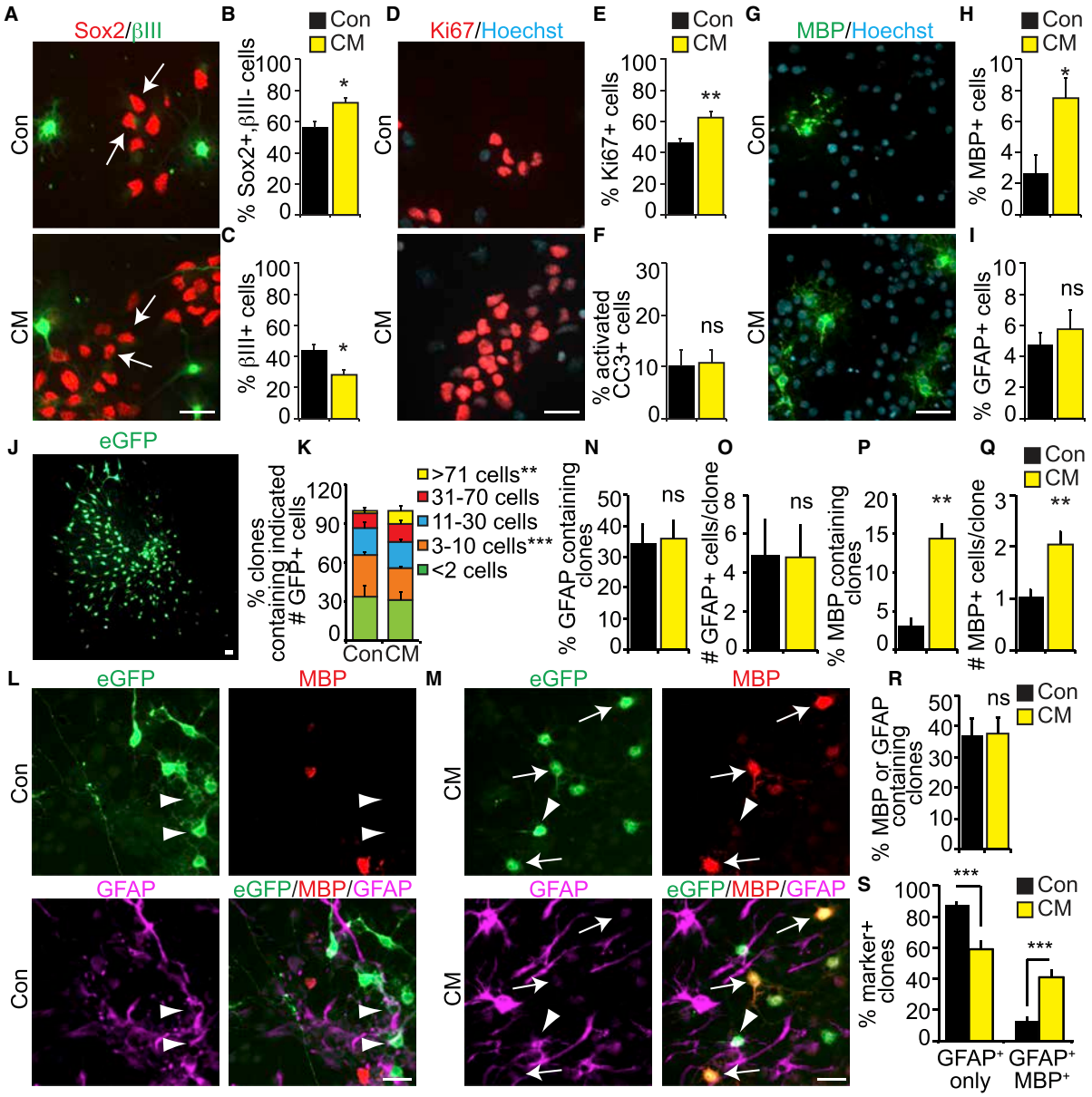

Figure 2. MGE Interneuron CM Increases Cortical Precursor Proliferation and Oligodendrogenesis

(A–I) E13 cortical precursors were cultured in control medium (Con) or MGE interneuron CM (CM) for 2 (A–F) or 7 (G–I) days. (A–C) Cultures were immunostained for Sox2 (red, A, arrows) and βIII-tubulin (green, A) and immunopositive cells were quantified (B and C). *$p < 0.05$; n = 3. (D–F) Cultures were immunostained for Ki67 (red, D) or cleaved caspase-3 (CC3), counterstained with Hoechst (blue, D) and immunopositive cells quantified (E and F). **$p < 0.01$; ns, not significant; n = 3. (G–I) 7 day cultures were immunostained for MBP (green, G) or GFAP, counterstained with Hoechst (blue, G), and immunopositive cells quantified. *$p < 0.05$; ns, nonsignificant. n = 3 experiments.

(J and K) E13 cortical precursors were transfected with PB-eGFP and PB-transposase and treated with control medium (Con) or CM for 7 days, immunostained for eGFP (J, representative large clone is shown), and the percentage size distribution was determined (K). **$p < 0.01$, ***$p < 0.001$; n = 4.

(L–S) PB-transfected E13 precursors were treated with control medium (L) or CM (M) for 7 days, immunostained for eGFP (green, L and M), MBP (red, L and M) and GFAP (magenta, L and M) and the percentages of eGFP-positive clones containing cells immunopositive for GFAP (N), MBP (P), and either GFAP or MBP (R) were determined. Also determined were the numbers of immunopositive cells per clone (O and Q), the percentage of clones containing both GFAP-positive and MBP-positive cells (GFAP+MBP+), and the percentage of clones containing only GFAP-positive cells (GFAP+ only) (S). Arrows and arrowheads in (L and M) denote eGFP-positive, MBP-positive oligodendrocytes and eGFP-positive, GFAP-positive astrocytes, respectively. **$p < 0.01$, ***$p < 0.001$; ns, not significant; $n \geq 3$. Scale bars, 20 μm. Error bars represent SEM.

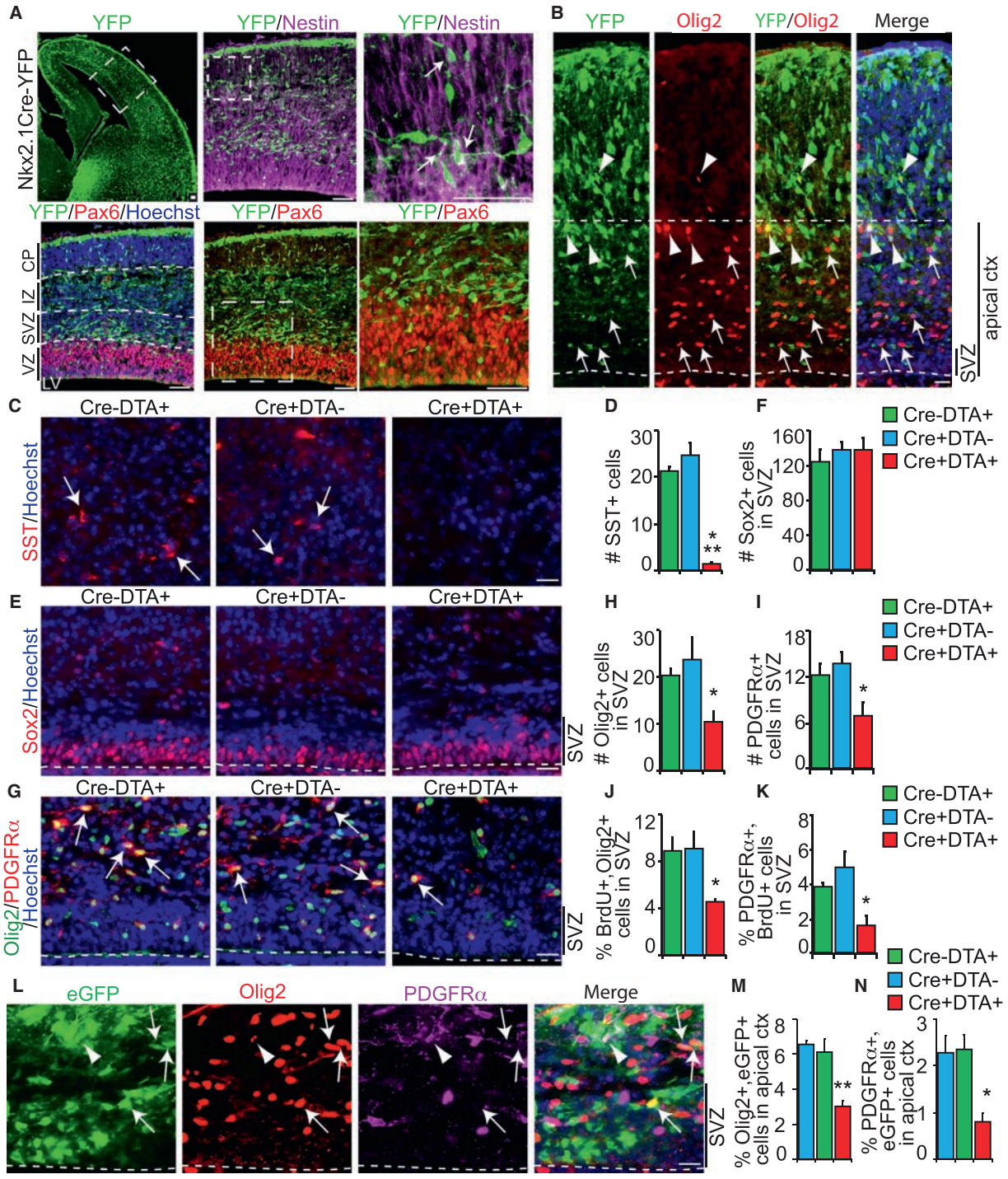

Figure 3. MGE Interneurons Regulate the Genesis of Cortical Oligodendrocyte Precursors In Vivo

(A and B) Images of coronal forebrain sections from E15 (A) or P0 (B) Nkx2.1Cre-positive, YFP^{stop}-positive embryos, immunostained for YFP (green) and Pax6 (red, bottom images, A), Nestin (magenta, top images, A) or Olig2 (red, B). In (A), the top left image hatched box shows the cortical region analyzed, and the middle image hatched boxes are shown to the right at higher magnification. Arrows denote YFP-positive MGE cells close to Nestin-positive precursor processes. In (B),

(legend continued on next page)

cortices (Figures 3C and 3D). In contrast, the number of Sox2-positive SVZ precursors was similar in all groups (Figures 3E and 3F). We also asked about oligodendrogenesis by immunostaining for two OPC markers, Olig2 and PDGFRα (Figure 3G). In all groups, Olig2-positive cells were scattered throughout the SVZ and adjacent cortex, with some coexpressing PDGFRα. However, there were about 2-fold fewer Olig2- and PDGFRα-positive cells in the SVZ of Nkx2.1-Cre; DTA^{stop} cortices (Figures 3H and 3I). Similar results were obtained when cortices were immunostained for BrdU and Olig2 or PDGFRα (Figures 3J and 3K).

To definitively establish that MGE interneurons are important for cortical oligodendrogenesis, we permanently tagged a subpopulation of cortical radial precursors in E14 Nkx2.1-Cre; DTA^{stop} mice by in utero electroporation of the PB eGFP reporter and transposase. As controls, we performed similar electroporations with Nkx2.1-Cre or DTA^{stop} embryos. We analyzed these cortices by counting eGFP-positive cells expressing Olig2 or PDGFRα in the apical cortex, which includes the SVZ and presumptive corpus callosum and which contains most oligodendrocyte lineage cells at this stage (see Figure S1B) (Ivanova et al., 2003; Kessaris et al., 2006). There were significantly fewer eGFP-positive cells expressing Olig2 or PDGFRα in Nkx2.1-Cre; DTA^{stop} apical cortices (Figures 3L–3N), confirming that MGE-derived progeny are essential for normal cortical oligodendrogenesis.

Fractalkine Secreted by MGE Interneurons Is Necessary and Sufficient to Promote Cortical Oligodendrogenesis in Culture

These data suggest that MGE interneurons secrete factors to promote cortical oligodendrogenesis. To identify ligands and receptors mediating the observed effects, we defined potential paracrine interactions using transcriptome data. For ligands, we performed a microarray analysis of RNA from three independent isolates of cultured MGE neurons. We extracted the ligand mRNAs using a curated database of secreted factors (Yuzwa et al., 2016) with a cut-off of 40% of the highest log2 expression values. This analysis yielded 90 potential secreted ligands expressed by MGE interneurons (Table S1). For receptors, we used a microarray dataset from E13 cortical precursors (Yuzwa et al., 2016) and extracted receptor mRNAs using a curated receptor database (Yuzwa et al., 2016) and the same expression cut-off. We used these MGE neuron ligands and cortical precursor receptors to construct a paracrine interaction model with 51 potential ligand-receptor interactions (Figure 4A).

We focused on three candidate interneuron-secreted ligands within this model; VEGFA and Gas6, which have been reported to regulate cortical precursor self-renewal and oligodendrocyte biology, respectively (Zhu et al., 2003; Goudarzi et al., 2016; Shankar et al., 2006), and fractalkine (or CX3CL1), which is not known to regulate developing CNS precursors or oligodendrocytes but has previously been implicated in myelination from a microglial perspective (Garcia et al., 2013; Lampron et al., 2015). We cultured E13 cortical precursors in varying concentrations of the three ligands for 2 or 7 days. Immunostaining after 2 days showed that none of the factors affected Sox2-positive precursors or βIII-tubulin-positive neurons (Figures 4B and 4C). However, analysis at 7 days showed that fractalkine and Gas6, but not VEGFA, significantly increased MBP-positive oligodendrocytes in a concentration-dependent fashion without affecting GFAP-positive astrocytes (Figures 4D–4F).

Consistent with the idea that fractalkine and Gas6 are potentially important interneuron-secreted ligands, ELISAs showed that both ligands were present in MGE interneuron CM (Figure 4G). We therefore asked whether blocking fractalkine or Gas6 activity abrogated the oligodendrogenic effects of interneuron CM using previously characterized function-blocking antibodies to fractalkine (Robinson et al., 2000), the fractalkine receptor (CX3CR1) (Furuichi et al., 2006; Robinson et al., 2000), or to the three Gas6 receptors, Tyro3, Axl, and Mertk (collectively termed TAM) (Park et al., 2012). Analysis of E13 cortical precursors cultured in interneuron CM for 7 days showed that antibodies to fractalkine or its CX3CR1 receptor, but not those for the Gas6 receptors or a control IgG, completely blocked the CM-mediated increase in MBP-positive oligodendrocytes (Figure 4H).

A number of additional experiments demonstrated the specificity of these effects. First, antibodies to fractalkine or its receptor had no effect on survival of MBP-positive oligodendrocytes, although anti-TAM increased the proportion of MBP-positive cells with condensed, apoptotic nuclei (Figure 4I; Figure S2), consistent with previous findings (Binder et al., 2008; Shankar et al., 2006). Second, GFAP-positive astrocytes were unaffected by CM with or without anti-fractalkine or anti-CX3CR1 (Figure 4J). Finally, both anti-fractalkine and anti-CX3CR1 inhibited the increase in MBP-positive cells caused by exogenous fractalkine (Figure 4K).

arrows denote YFP-negative, Olig2-positive cortical cells, and arrowheads YFP-positive, Olig2-positive MGE-derived cells. LV, lateral ventricle. In (B), hatched lines define the apical cortex (apical ctx).

(C–K) P0 Nkx2.1Cre-negative, DTA^{stop}-positive (Cre-DTA+), Nkx2.1Cre-positive, DTA^{stop}-negative (Cre+DTA-), and Nkx2.1Cre-positive, DTA^{stop}-positive (Cre+DTA+) cortices were analyzed by immunostaining. Some mice were exposed to a maternal BrdU injection at E18.5. (C–F) Sections were immunostained for somatostatin (red, SST, C, arrows) or Sox2 (red, E) and quantified for somatostatin-positive cells in the cortex (D) or Sox2-positive cells in the SVZ (F). ***$p < 0.001$; $n \geq 3$ mice per group. (G–K) Sections were immunostained for Olig2 (green, G), PDGFRα (red, G) and quantified for Olig2-positive (H) and PDGFRα-positive (I) cells in the SVZ. In (J) and (K) sections were also immunostained for BrdU (Figure S1A), and BrdU-positive cells that also expressed Olig2 (J) or PDGFRα (K) were quantified in the same way. Hatched lines in (E) and (G) denote the apical cortical border. *$p < 0.05$; $n \geq 3$ mice per group.

(L–N) Cortices of the same groups of mice as in (C–K) were electroporated in utero at E14 with PB-eGFP and PB-transposase, immunostained at E18.5 for eGFP (green, L), Olig2 (red, L), and PDGFRα (magenta, L) and apical cortices (apical ctx, see Figure S1B) were quantified for the percentages of eGFP-positive cells that were positive for Olig2 (M) or PDGFRα (N). *$p < 0.05$, **$p < 0.01$; $n \geq 3$ mice per group. Arrows and arrowheads in (L) denote eGFP-positive, Olig2-positive cells that were negative and positive for PDGFRα, respectively. Some images also show Hoechst counterstaining (blue), as indicated. Scale bars, 20 μm, except in (A), 50 μm. Error bars represent SEM. Also see Figure S1.

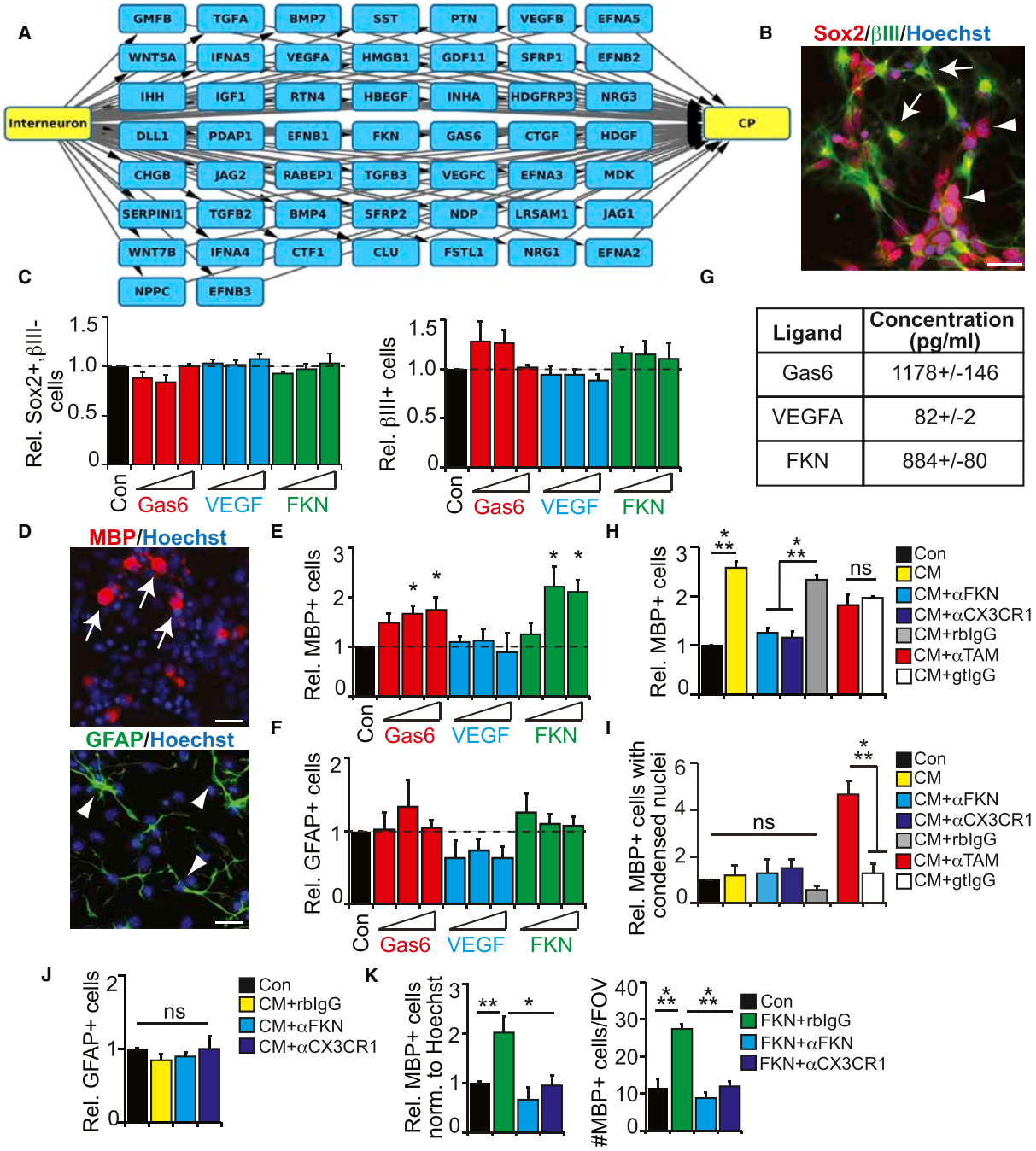

Figure 4. Fractalkine Mediates MGE Interneuron-Induced Cortical Oligodendrogenesis in Culture

(A) Transcriptome-based network model of MGE interneuron and cortical precursor communication. MGE interneuron RNA was analyzed using Affymetrix GeneChip Mouse Gene 2.0 ST Arrays (GEO: GSE95696) and ligand mRNAs extracted, while receptor mRNAs were extracted from previously published microarray data (Yuzwa et al., 2016; GEO: GSE84482). In both cases, a cut-off threshold of 40% of the highest log2 expression values were used, and relevant ligands and receptors were matched using a curated ligand-receptor database (Yuzwa et al., 2016). Nodes in blue between interneuron and cortical precursor (CP) nodes (yellow) represent ligands predicted to act in a paracrine fashion on cortical precursors.

(legend continued on next page)

Fractalkine Promotes Oligodendrocytic Differentiation of Cultured Gliogenic Precursors

To ask how fractalkine promotes oligodendrogenesis, we first characterized expression of the fractalkine receptor CX3CR1 on cultured cortical precursors, using double-label single molecule fluorescent in situ hybridization (FISH). At 2 days in culture, when neurons are generated, *Cx3cr1* mRNA was expressed in a small subset of *Sox2*-positive precursors (Figure 5A). By 6 days, about half of the total cells expressed *Olig2* mRNA and almost all of these (>95%) were also positive for *Cx3cr1* mRNA (Figure 5B). Fewer cells were positive for *Pdgfrα*, but almost all of these were also *Cx3cr1* positive (Figure 5C). In addition, some *Cx3cr1*-positive cells were negative for *Olig2* and *PDGFRα* mRNAs but positive for *Sox2* mRNA (Figures 5B and 5C; Figure S3A), potentially representing an earlier gliogenic precursor. We ensured the specificity of the FISH using non-specific probes (Figure S3B).

To ask whether fractalkine enhanced oligodendrogenesis by promoting gliogenic precursor proliferation, we added BrdU to cortical precursor cultures at 1 or 4 days and characterized BrdU-positive cells 24 hr later. Fractalkine had no effect on total BrdU-positive cells at either time point (Figures 5D, 5E, and 5G). To ask more specifically about gliogenic precursors, we added BrdU at 4 days and immunostained 1 day later for BrdU, Olig2, and PDGFRα (Figure 5F). While fractalkine significantly increased total PDGFRα-positive cells, it had no effect on the proportion of Olig2-positive or PDGFRα-positive cells that were also BrdU-positive (Figures 5H–5J).

To ask whether fractalkine increases oligodendroglial differentiation without affecting proliferation, we performed clonal analysis using the PB reporter system. Immunostaining of PB-transfected cultures after 7 days showed that fractalkine significantly increased the proportions of clones containing MBP- or O4-positive oligodendrocytes but that it had no effect on the number of MBP- or O4-positive oligodendrocytes per clone (Figures 5K and 5L). We obtained similar results analyzing OPCs at 5 days post-plating. Fractalkine significantly increased the proportions of clones containing Olig2- or PDGFRα-positive cells without affecting the number of positive cells per clone (Figures 5M–5O).

Finally, we asked whether fractalkine affected postnatal OPCs, culturing neonatal glial cells enriched for OPCs (O'Meara et al., 2011). When these cultures were incubated in proliferation medium and pulsed with BrdU on day 2 for 16 hr, fractalkine had no effect on the proportion of Olig2-positive cells that were BrdU-positive (Figure 5P; Figure S3C). In contrast, when these cultures were incubated in differentiation medium and analyzed on day 4, fractalkine significantly increased the proportion of Olig2-positive cells that also expressed MBP (Figure 5Q; Figure S3D). Thus, fractalkine enhances the oligodendroglial differentiation of both embryonic and postnatal glial precursors without affecting their proliferation.

Expression of the Fractalkine Receptor, CX3CR1, in Gliogenic Precursors and Fractalkine in MGE Interneurons in the Developing Cortex

To ask whether fractalkine also regulated oligodendrogenesis in vivo, we analyzed *Fractalkine* and *Cx3cr1* mRNAs in the developing cortex. Quantitative RT-PCR (Figure 6A) showed that both mRNAs were most robustly expressed in the postnatal cortex during the period of oligodendrocyte formation. We then asked what cell types expressed these mRNAs using FISH. At E15 (Figures S4A and S4B), *Cx3cr1* and *Olig2* mRNAs were only expressed in scattered VZ/SVZ cells, while *Sox2* mRNA was abundantly expressed in cells in this region. By E17 (Figure 6B; Figure S4C), *Olig2* mRNA was expressed in a subpopulation of cells in the basal VZ and SVZ, and almost all of these coexpressed *Cx3cr1* and *Sox2* mRNAs. By P4 (Figure 6C; Figure S4D), *Cx3cr1* mRNA was robustly expressed in the SVZ and in a band of cells basal to the SVZ. Many of these were *Olig2* positive or *Sox2* positive, and some were both. Double-label FISH for *Cx3cr1* and *Pdgfrα* mRNAs at this same time point (Figure 6D) showed that *Pdgfrα* mRNA was expressed in scattered cells throughout the cortex and that *Cx3cr1* mRNA was coexpressed in the *Pdgfrα*-positive cells within and basal to the SVZ. At all time points, we observed occasional cells that robustly expressed only *Cx3cr1* mRNA. Immunostaining identified these as Iba1-positive microglia (Figure S4E), known to express high levels of CX3CR1 (Lampron et al., 2015).

We also asked about fractalkine expression. FISH at E17 (Figure 6E), showed that *Fkn* mRNA was expressed in cells of the VZ/SVZ and that many of these coexpressed low levels of *Somatostatin* (*Sst*) mRNA. By P4 (Figures 6F and 6G), almost all *Sst*-positive interneurons (about 95%) coexpressed *Fkn* mRNA, and some of these were closely apposed to *Pdgfrα*-positive OPCs (Figure 6H). There were also many *Fkn*-positive, *Sst*-negative cells in the CP at this time point, potentially cortical neurons. We confirmed expression of *Fkn* mRNA in MGE interneurons by performing FISH on Nkx2.1-Cre;YFP^{stop} cortices. At E15, *Fkn* mRNA was detectable in YFP-positive, MGE-derived cells (Figure 6I; Figure S4F) and by P0 almost all YFP-positive cortical

(B–F) E13 cortical precursors were cultured in vehicle (Con) or increasing concentrations of Gas6 (50, 100 and 250 ng/mL), VEGF (10, 50, and 100 ng/mL) or fractalkine (FKN; 100, 250, and 500 ng/mL) for 2 days (B and C) or 7 days (D–F), and immunostained for βIII-tubulin (green, B, arrows) and Sox2 (red, B, arrowheads), or for MBP (red, D, arrows) or GFAP (green, D, arrowheads). The proportions of immunopositive cells were expressed relative to total Hoechst-positive cells (B and D, blue) and normalized to vehicle. *$p < 0.05$. n = 3 experiments.

(G) ELISA analysis for Gas6, VEGFA, and fractalkine (FKN) in MGE interneuron CM, shown in pg/mL ± SEM, n = 3 CM preparations.

(H–J) E13 cortical precursors were cultured 7 days in control medium (Con) or MGE interneuron CM with non-specific rabbit IgG (CM+rbIgG), non-specific goat IgG (CM+gtIgG), or with function-blocking antibodies for fractalkine (CM+αFKN), CX3CR1 (CM+αCX3CR1), or for the Gas6 receptors Tyro3, Mertk, and Axl (CM+ αTAM). Cultures were immmunostained for MBP (H and I) or GFAP (J), and counterstained with Hoechst. In (H) and (J), the proportions of immunopositive cells were expressed relative to total Hoechst-positive cells and normalized to vehicle. In (I), the proportion of MBP-positive cells with condensed apoptotic nuclei (Figure S2) was determined and normalized to vehicle. ***$p < 0.001$; ns, not significant; n = 3.

(K) Analysis of cultures as in (H)–(J) except that they were grown in exogenous fractalkine (FKN; 250 ng/mL) rather than CM. Data are expressed relative to total Hoechst-positive cells and normalized to the control (left panel) or as absolute numbers per field of view (right panel). *$p < 0.05$; **$p < 0.01$, ***$p < 0.001$; n = 3. Scale bars, 20 μm. Error bars represent SEM. Also see Figure S2.

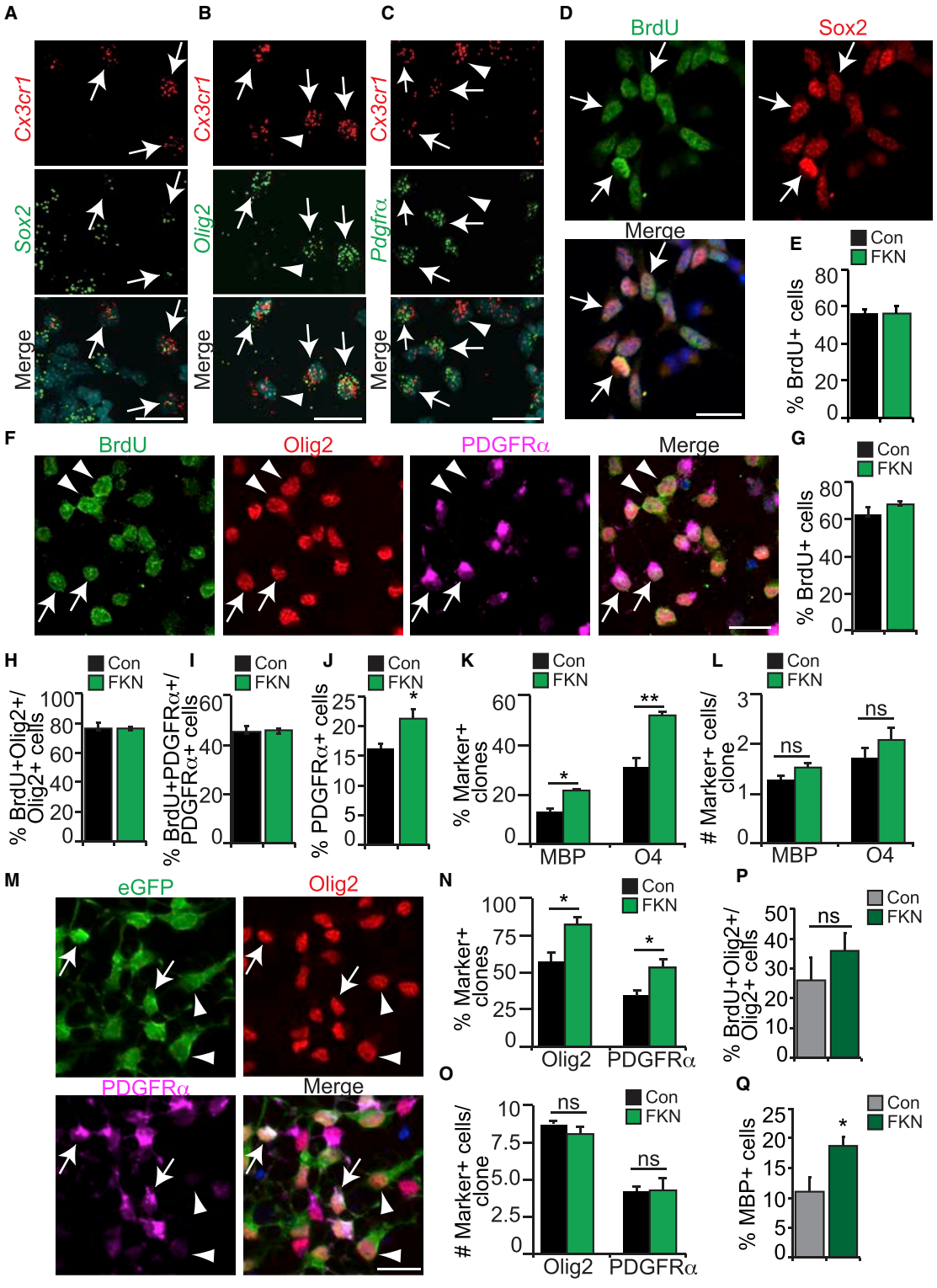

(legend on next page)

cells were positive for *Fkn* mRNA (Figure 6J). Analysis of MGE interneuron cultures confirmed that virtually all Gad67-positive interneurons expressed *Fkn* mRNA (Figure 6K).

We performed one final experiment to ask about the relative importance of interneurons as a source of Fractalkine for cortical precursors. Specifically, we performed FISH on E18.5 Nkx2.1-Cre; DTA^{stop} cortices that were electroporated with PB-eGFP at E14, comparing it to similarly electroporated DTA^{stop} or Nkx2.1-Cre cortices. There were 2- to 3-fold fewer *Fkn* mRNA-positive cells in the SVZ of Nkx2.1-Cre; DTA^{stop} mice (Figure 6L; Figure S4G). Thus, MGE interneurons are a major source of Fractalkine in the SVZ during gliogenesis.

The Fractalkine Receptor, CX3CR1, Is Necessary for Cortical Oligodendrogenesis

To test the idea that fractalkine is important for cortical oligodendrogenesis, we examined mice with a constitutive knockout of CX3CR1 (Jung et al., 2000). Immunostaining of P0 cortices demonstrated a 35% reduction in Olig2-positive cells within the apical cortex of CX3CR1$^{-/-}$ mice, as well as a significant decrease even in the heterozygous CX3CR1$^{+/-}$ mice (Figures 7A and 7B; see Figure S1A). To ask whether these decreases were caused by deficits in proliferating gliogenic precursors, we analyzed sections for Ki67 (Figure 7C). In the CX3CR1$^{-/-}$ apical cortex, total Ki67-positive cells were reduced (Figure 7D). This was due to an almost 2-fold decrease in Olig2-positive, Ki67-positive cells (Figure 7E), since Olig2-negative, Ki67-positive cells (presumably Sox2-positive cortical precursors) were unaffected (CX3CR1$^{+/+}$, 46.7 ± 6.0; CX3CR1$^{+/-}$, 45.3 ± 5.9; CX3CR1$^{-/-}$, 36.3 ± 0.9 cells in the apical cortex, $p > 0.05$). We observed a similar decrease in PDGFRα-positive, Ki67-positive cells in the CX3CR1$^{-/-}$ apical cortex (Figures 7F–7H). However, in spite of these decreases in total proliferating OPCs, loss of one or two alleles of the *Cx3cr1* gene had no effect on the relative proliferation index of Olig2-positive cells (Figure S5A).

We also characterized the cortex at P15, when oligodendrocytes had been generated and myelination was taking place. Immunostaining for CC1, which is expressed in oligodendrocytes but not OPCs, and for Olig2 demonstrated that both OPCs (Olig2 positive, CC1 negative) and oligodendrocytes (Olig2 positive, CC1 positive) were significantly decreased in the corpus callosum and gray matter of CX3CR1$^{-/-}$ cortices (Figures 7I–7M; Figure S5B). In contrast, glutamine synthetase-positive astrocyte numbers were similar between genotypes in these regions (Figures 7N–7P).

One potential caveat is that our various manipulations might alter microglia, which express high levels of CX3CR1, thereby indirectly causing the observed phenotypes. We therefore characterized microglia in our various models. Analysis of control cortices showed that there were relatively few Iba1-positive microglia at P0, with many more at P15, and that the locations and numbers of these were unaffected by constitutive knockout of CX3CR1 (Figures 7Q and 7R; Figures S5C–S5E). A similar analysis of E18.5 Nkx2.1-Cre; DTA^{stop} cortices that were electroporated with PB-eGFP at E14 showed that none of the microglia were eGFP-positive (as predicted since the electroporation only targets radial precursor cells and their progeny) and that microglial numbers and location were unaffected by the loss of MGE interneurons in these mice (Figure 7S; Figures S5F and S5G).

Fractalkine Acts through CX3CR1 in Cortical Precursors to Regulate Cortical Oligodendrogenesis

To definitively ask whether CX3CR1 is required in cortical precursors for oligodendrogenesis, we performed shRNA-mediated knockdowns. To do this, we generated several CX3CR1 shRNAs in a PB transposon backbone that contains a tGFP cassette to ensure genomic integration and expression throughout the postnatal period of oligodendrogenesis. As controls, we used a scrambled shRNA or a Luciferase shRNA in the same backbone. Transfection into HEK293 cells demonstrated that both CX3CR1 shRNAs specifically and efficiently knocked down murine CX3CR1 (Figures 8A and 8B). We then asked whether they were also efficacious in cortical precursors, by cotransfecting them into E13 cortical cultures together with the PB transposase, and culturing cells for 7 days with or without fractalkine. The CX3CR1 shRNAs inhibited the fractalkine-induced increase in oligodendrocytes expressing MBP or a second marker, O4,

Figure 5. Fractalkine Enhances Oligodendroglial Differentiation without Affecting Proliferation

(A–C) E13 cortical precursors were cultured for 2 days (A) or 6 days (B and C) and analyzed by FISH for *Cx3cr1* (red) and *Sox2* (green, A), *Olig2* (green, B), or *Pdgfrα* (green, C) mRNAs. Cultures were counterstained with Hoechst (blue in merges). Arrows and arrowheads denote double- and single-positive cells, respectively.

(D–J) E13 cortical precursors were cultured in vehicle (Con) or fractalkine (FKN; 250 ng/mL), and BrdU was added either 1 day (D and E) or 4 days (F–J) post-plating. Cells were immunostained 24 hr post-BrdU for BrdU (green, D and F) and Sox2 (red, D) or Olig2 (red, F) and PDGFRα (magenta, F) and quantified for the percentage of total cells that were BrdU positive (E and G) or PDGFRα positive (J), or for the percentage of Olig2-positive or PDGFRα-positive cells that were also positive for BrdU (H and I). Arrows denote double- or triple-positive cells, while arrowheads in (F) indicate BrdU-positive, Olig2-positive, PDGFRα-negative cells. *$p < 0.05$; $n = 3$.

(K and L) E13 cortical precursors were transfected with PB-eGFP and PB-transposase, cultured 7 days in vehicle (Con) or fractalkine (FKN; 250 ng/mL), immunostained for eGFP, MBP and O4, and quantified for the percentage of eGFP-positive clones that contained at least one MBP-positive or O4-positive cell (K). Also quantified were the mean numbers of MBP-positive or O4-positive cells per clone. (L). *$p < 0.05$, **$p < 0.01$, ns = not significant; $n = 3$.

(M–O) E13 cortical precursors were transfected and cultured as in (K) and (L) for 5 days, were immunostained for eGFP (green, M), Olig2 (red, M) and PDGFRα (magenta, M) and quantified for the percentage of eGFP-positive clones containing at least one Olig2-positive or PDGFRα-positive cell (N) and for the mean number of Olig2-positive or PDGFRα-positive cells per clone (O). *$p < 0.05$, ns = not significant; $n = 3$. Arrows and arrowheads in (M) denote eGFP-positive, Olig2-positive cells that do or do not express PDGFRα, respectively.

(P and Q) P0 enriched glial cultures were cultured with vehicle (Con) or 250 ng/mL fractalkine (FKN) for 2 days in proliferation medium, BrdU was added, 16 hr later cultures were immunostained for BrdU and Olig2, and the proportion of Olig2-positive cells that were also BrdU-positive was determined (P; Figure S3C). Alternatively, cells were cultured 4 days in differentiation medium, and the percentage of MBP-positive cells quantified (Q; Figure S3D). *$p < 0.05$; ns, not significant; $n \geq 3$. All merged images also show the Hoechst counterstain (blue). Scale bars, 20 μm. Error bars represent SEM. Also see Figure S3.

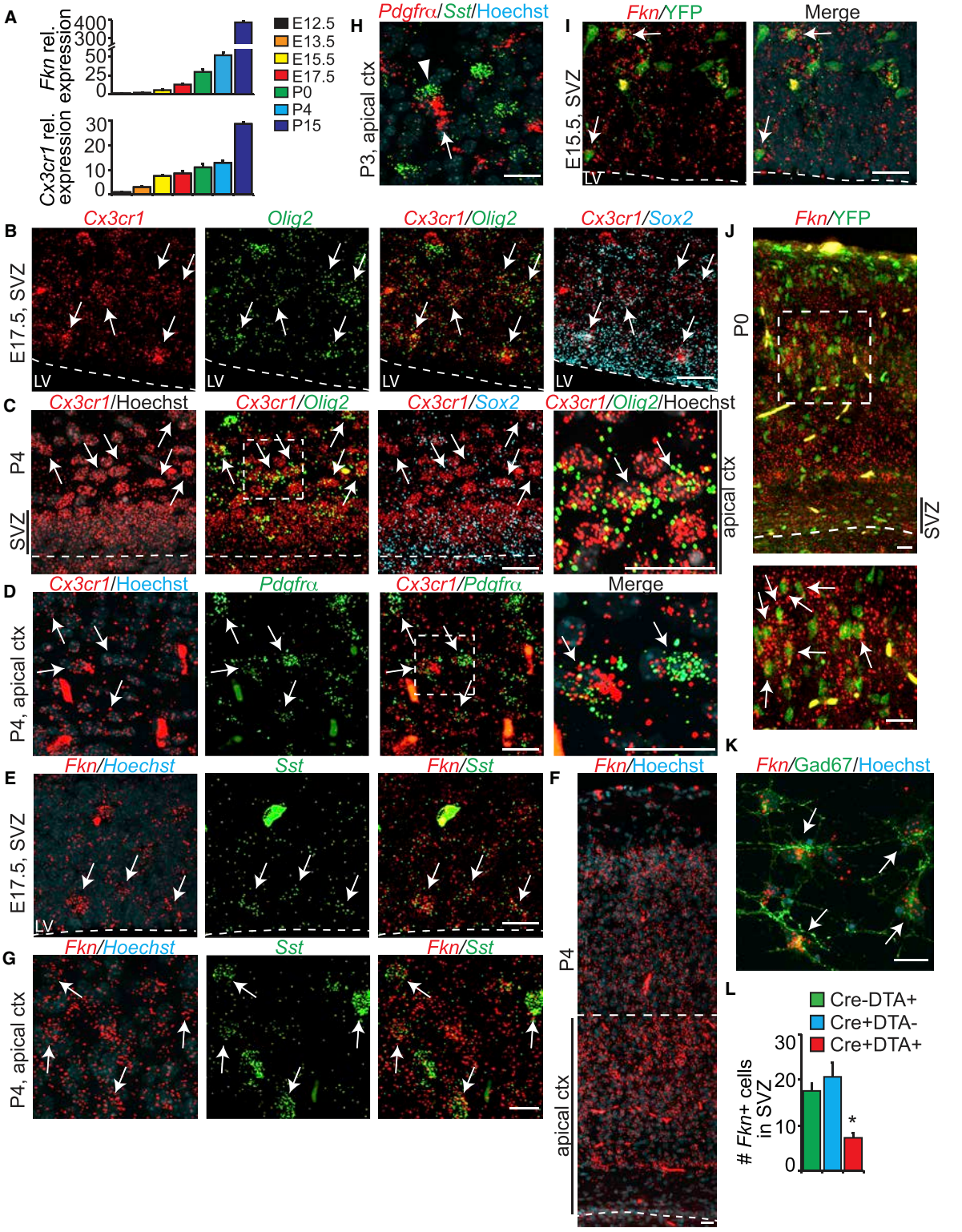

(legend on next page)

while the control shRNAs had no effect (Figures 8C and 8D; Figure S6A).

We also confirmed the specificity of the knockdowns by performing rescue experiments with a human CX3CR1 expression plasmid that was not targeted by the shRNAs. Specifically, we co-transfected E13 cortical precursors with control or murine CX3CR1 shRNAs and the PB transposase, as well as the human CX3CR1 expression plasmid, and then cultured these cells with added fractalkine. Analysis at 7 days showed that fractalkine caused an increase in O4-positive cells, that this was specifically blocked by the CX3CR1 shRNAs, and that coincident expression of human CX3CR1 rescued this effect (Figures 8E and 8F).

We then used the most efficacious of these two shRNAs (shRNA2) to knockdown CX3CR1 in vivo by electroporating E14 cortices with the PB transposase and either control or CX3CR1 shRNAs. Immunostaining at P15 for tGFP, Olig2, and CC1 (Figures 8G and 8I) demonstrated that CX3CR1 knockdown caused a modest decrease in tGFP-positive cells in the corpus callosum and a coincident increase in the cortical layers (Figure 8H). This change in cellular localization was accompanied by a significant decrease in tGFP-positive OPCs and oligodendrocytes in the corpus callosum (Figures 8J and 8K; Figure S6B). In contrast, the proportions of tGFP-positive, glutamine synthetase-positive astrocytes in the corpus callosum or gray matter were unaffected by CX3CR1 knockdown (Figures 8L–8N).

To ask whether these decreases in oligodendrocyte lineage cells reflected a developmental deficit in oligodendrogenesis, we performed a similar analysis on electroporated cortices that were harvested at P0 (Figure 8O). This analysis showed that CX3CR1 knockdown caused a 37% decrease in tGFP-positive, Olig2-positive glially biased precursors in the apical cortex (Figure 8P). Moreover, there were approximately 2-fold fewer tGFP-positive cells expressing Ki67 alone or Ki67 and Olig2 (Figures 8Q and 8R). However, the proliferation index of Olig2-positive cells was unaffected (Figure S6C). As a control, we confirmed that none of the tGFP-positive cells were positive for Iba1 (Figure S5D) and that numbers and locations of microglia were unaffected (Figures 8S and 8T). Thus, CX3CR1 knockdown in embryonic cortical precursors causes them to generate only about half as many oligodendrocyte lineage cells.

DISCUSSION

The developmental genesis of neurons and glia results from a complex interplay between mechanisms intrinsic to neural precursors and extrinsic cues within their environment. This environment is defined, in part, by neural precursors themselves, and by newborn cortical neurons, the first cell type to be made during embryogenesis (Yuzwa et al., 2016; Barnabé-Heider et al., 2005). However, neural precursors and excitatory neurons are not the only cell types present in the developing cortex. In particular, embryonic interneurons are generated in the adjacent ganglionic eminences and then migrate into the cortex where some of them associate closely with cortical precursors (Yokota et al., 2007). Here, we show that these migratory interneurons are essential for normal oligodendrogenesis, a function that they fulfill by secreting fractalkine.

Within the murine cortex, radial precursor cells generate neurons from about E11 to E17/18 and then start to make glia, with astrocytes first made immediately prior to birth and the first oligodendrocytes postnatally (Gauthier-Fisher and Miller, 2013). These same radial precursors also generate two precursor populations that persist into adulthood, a subpopulation of adult SVZ neural stem cells, and adult OPCs. With regard to this time course, our data support a model where newborn MGE interneurons interact with and regulate cortical precursors from about E14, when they first arrive in the precursor and intermediate migratory zones, through the postnatal period of oligodendrocyte genesis. We propose that these newly arrived interneurons secrete fractalkine that acts directly upon glially biased cortical precursors and OPCs to promote oligodendroglial differentiation throughout at least the first few weeks of postnatal life. Our data indicate that fractalkine mediates this pro-oligodendrogenic effect by enhancing differentiation of glial precursors without affecting proliferation. In this regard, the Olig2 transcription factor was recently shown to associate with the *Cx3cr1* gene in postnatal OPCs, but not in oligodendrocytes (Yu et al., 2013). This would explain why CX3CR1 is expressed in almost all Olig2-positive cortical cells and suggests that an Olig2-CX3CR1 regulatory loop might be a key determinant of successful oligodendroglial differentiation.

Figure 6. Fractalkine Is Expressed in MGE Interneurons, and CX3CR1 Is Expressed in Cortical Oligodendrocyte Precursor Cells

(A) qRT-PCR for *Fkn* and *Cx3cr1* mRNAs in cortices from E12.5 to P15. Data were normalized to *Gapdh* mRNA and expressed relative to E12.5 values. n = 3 mice each.

(B and C) Triple-label FISH of E17.5 (B, Figure S4C) and P4 (C, Figure S4D) cortices for *Cx3cr1* (red), *Olig2* (green) and *Sox2* (blue) mRNAs. Arrows denote *Cx3cr1*-positive, *Olig2*-positive cells. The hatched box in (C) is shown at higher magnification to the right.

(D) Double-label FISH for *Cx3cr1* (red) and *Pdgfrα* (green) mRNAs in the P4 apical cortex region. The boxed area is shown at higher magnification to the right. Arrows denote double-labeled cells.

(E–G) FISH of E17.5 (E) and P4 (F and G) cortices for *Fkn* (red) and *Sst* (green) mRNAs. Images in (G) are from the apical cortex. Arrows denote double-labeled cells.

(H) Double-label FISH for *Pdgfrα* (red) and *Sst* (green) mRNAs in the P3 apical cortex. The arrow and arrowhead indicate closely apposed *Pdgfrα*- and *Sst*-positive cells.

(I) FISH for *Fkn* mRNA (red) in the E15.5 Nkx2.1Cre-positive, YFP^{stop}-positive cortical SVZ (also see Figure S4F). YFP was directly visualized (green). Arrows indicate *Fkn*-positive, YFP-positive cells.

(J) FISH for *Fkn* mRNA (red) in the P0 Nkx2.1Cre-positive, YFP^{stop}-positive cortex. YFP was directly visualized (green). The hatched box is shown at higher magnification in the bottom image. Arrows indicate *Fkn*-positive, YFP-positive cells.

(K) FISH for *Fkn* mRNA (red) in cultures of MGE interneurons immunostained for Gad67 (green). Arrows denote *Fkn*-positive, Gad67-positive cells.

(L) Quantification of the mean number of cells containing three or more *Fkn* mRNA foci in the cortical SVZ of E18 Nkx2.1Cre-negative, DTA-positive (Cre-DTA+), Nkx2.1Cre-positive, DTA-negative (Cre+DTA-), and Nkx2.1Cre-positive, DTA-positive (Cre+DTA+) mice (see Figure S4G). *$p < 0.05$; $n \geq 3$ per group. In all images except (B), blue or gray shows Hoechst counterstaining. Scale bars, 20 μm. Error bars represent SEM. Also see Figure S4.

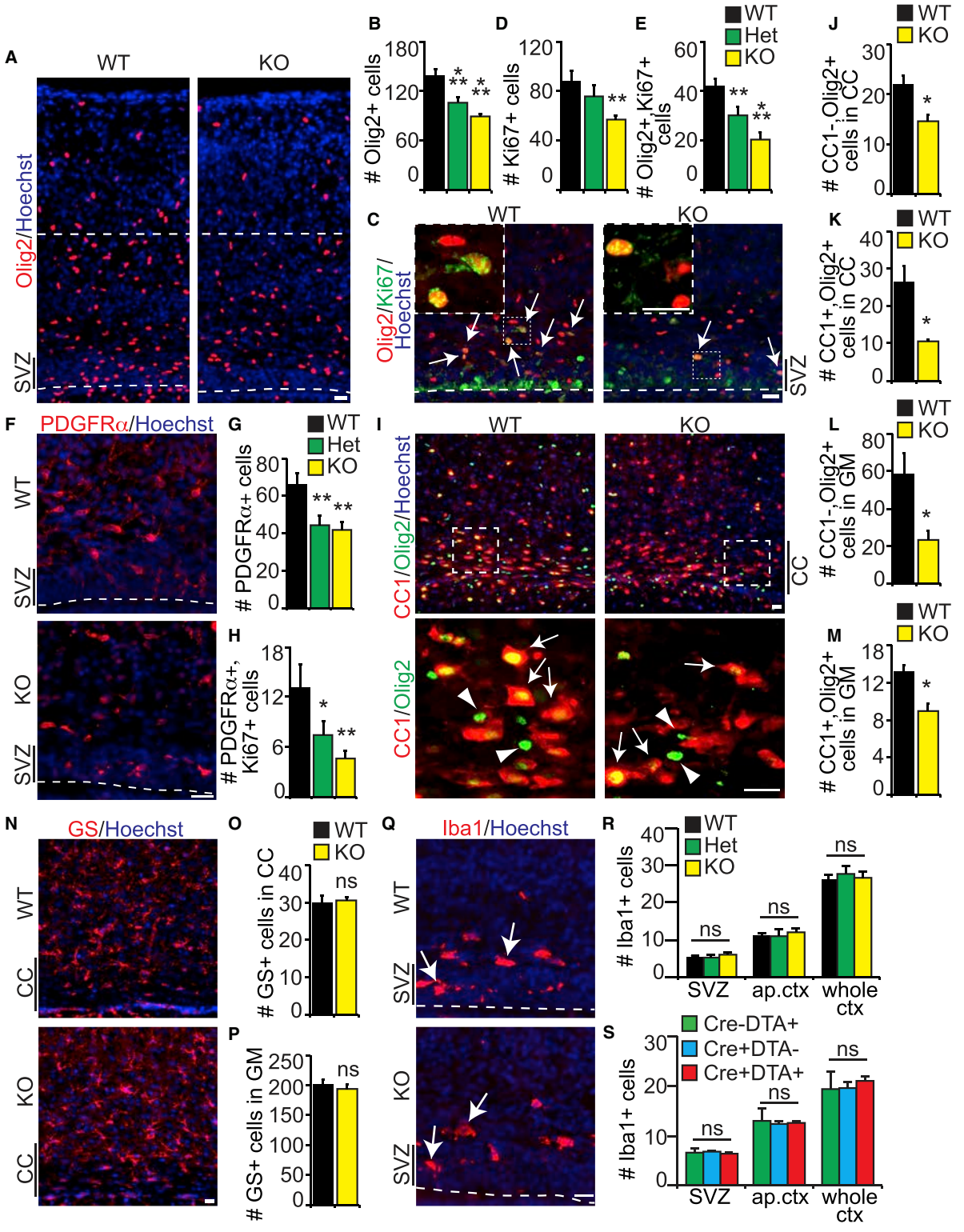

(legend on next page)

One key question raised by this model is whether interneuron-derived fractalkine regulates the genesis of oligodendrocytes throughout life, particularly since we show that it acts directly upon postnatal OPCs. In this regard, adult OPCs are closely associated with interneurons (Orduz et al., 2015), and parvalbumin-positive cortical interneurons are myelinated (Micheva et al., 2016), raising the possibility that they might secrete fractalkine to directly regulate their own myelination. A second key question involves the importance of fractalkine secreted by interneurons relative to other potential cellular sources. In this regard, our FISH data show that many non-MGE-derived cells within the cortical layers also express *Fkn* mRNA and we (Yuzwa et al., 2016) and others (Cook et al., 2010) have reported that cortical neurons express and secrete fractalkine. Thus, excitatory neurons might also secrete fractalkine to regulate axon-associated OPCs and/or oligodendrocytes. Intriguingly, the activity of forebrain neurons, including cortical projection neurons, has been shown to regulate oligodendrogenesis (Gibson et al., 2014; McKenzie et al., 2014), and it is tempting to speculate that axonally secreted fractalkine might be one of the factors that play a role in this process.

Almost all work on fractalkine in the CNS has focused on microglia, which express high levels of CX3CR1 (Limatola and Ransohoff, 2014; Sheridan and Murphy, 2013). While our experiments indicate that fractalkine directly regulates glial precursors, they do not rule out a potentially important role for microglia vis a vis oligodendrocytes. Intriguingly, a number of these studies have induced demyelination in CX3CR1$^{-/-}$ mice with cuprizone or experimental autoimmune encephalomyelitis (EAE) (Garcia et al., 2013; Lampron et al., 2015) and have observed aberrant remyelination coincident with reduced demyelination-induced recruitment of Olig2- and PDGFRα-positive OPCs into the corpus callosum (Lampron et al., 2015). While the CX3CR1$^{-/-}$ microglia were clearly aberrant in these studies, it is nonetheless tempting to speculate that the observed phenotypes were in part due to a deficit in oligodendrogenesis caused by the loss of fractalkine signaling in neural precursors and/or OPCs. It will also be interesting to see whether a recently reported deficit in developmental pruning and connectivity in the CX3CR1$^{-/-}$ forebrain (Zhan et al., 2014) might also be partially due to deficits in oligodendrogenesis.

Our findings may also have implications for glioma, since endogenous fractalkine is thought to negatively regulate glioma invasion (Sciumè et al., 2010). It is tempting to speculate that fractalkine secreted by interneurons might negatively affect Olig2-positive gliomas (Ligon et al., 2007; Lu et al., 2016) by promoting their differentiation down the oligodendroglial lineage. This would be in direct contrast to another neuronally produced ligand, neuroligin-3, which promotes glioma cell proliferation (Venkatesh et al., 2015).

In summary, we have defined an unexpected role for migrating interneurons in the developmental genesis of cortical oligodendrocytes, a role that they subserve by secreting fractalkine, a cytokine previously thought to act in the CNS only on microglia. Whether these findings reflect a general role for interneurons and/or fractalkine in oligodendrogenesis throughout the developing and adult brain remains a key question for the future.

STAR★METHODS

Detailed methods are provided in the online version of this paper and include the following:

- KEY RESOURCES TABLE
- CONTACT FOR REAGENT AND RESOURCE SHARING
- EXPERIMENTAL MODEL AND SUBJECT DETAILS
  - Mice
  - HEK293 cell cultures and transfections
  - MGE interneuron cultures
  - Conditioned medium preparation
  - Cortical precursor cell culture and transfections
  - Co-culture experiments
  - Postnatal OPC cultures
- METHOD DETAILS
  - Plasmids
  - Growth factors and function-blocking antibodies
  - Lineage tracing experiments
  - Genetic ablation experiments
  - In utero electroporations
  - Immunostaining
  - Antibodies
  - Fluorescent in situ hybridization (FISH)
  - Western blotting

Figure 7. Fractalkine Signaling Regulates the Genesis of Oligodendrocytes in the Developing Cortex

(A–H) P0 CX3CR1$^{+/+}$ (WT), CX3CR1$^{+/-}$ (Het) and CX3CR1$^{-/-}$ (KO) cortices were immunostained for Olig2 (red, A and C) or PDGFRα (red, F) with or without Ki67 (green, C), and the apical cortex (defined by hatched lines in A) was quantified for the number of cells positive for Olig2 (B), Ki67 (D), PDGFRα (G), or for Ki67-positive cells that also expressed Olig2 (E) or PDGFRα (H). *p < 0.05, **p < 0.01, ***p < 0.001; n = 3 mice each. In (C), arrows denote double-labeled cells, and the boxed regions are shown at higher magnification in the insets.

(I–P) P15 CX3CR1$^{+/+}$ (WT) and CX3CR1$^{-/-}$ (KO) cortices were immunostained for CC1 (red, I, also see Figure S5B) and Olig2 (green, I, also see Figure S5B) or for glutamine synthetase (GS, red, N), and the corpus callosum (CC) or cortical gray matter (GM) were quantified for Olig2-positive cells that were or were not positive for CC1 (J–M) or for glutamine synthetase-positive cells (O and P). The boxed regions in (I) are shown at higher magnification in the bottom panels, and the arrows and arrowheads denote CC1-positive, Olig2-positive oligodendrocytes and CC1-negative, Olig2-positive OPCs, respectively. *p < 0.05; ns, not significant; n = 3 mice each.

(Q and R) P0 CX3CR1$^{+/+}$ (WT), CX3CR1$^{+/-}$ (Het), and CX3CR1$^{-/-}$ (KO) cortices were immunostained for Iba1 (red, Q) and the numbers of microglia in the SVZ, apical cortex (ap. ctx) and whole cortex (whole ctx) were quantified (R). Also see Figures S5C–S5E. ns, not significant; n = 4 mice each. Arrows in (Q) denote Iba1-positive microglia.

(S) E18.5 Nkx2.1Cre-negative, DTA-positive (Cre-DTA+), Nkx2.1Cre-positive, DTA-negative (Cre+DTA-), and Nkx2.1Cre-positive, DTA-positive (Cre+DTA+) cortices were immunostained for Iba1 (see Figures S5F and S5G) and Iba1-positive cells in the SVZ, apical cortex (ap. ctx) and whole cortex (whole ctx) were quantified. ns, not significant; n ≥ 3 mice per group. In all images, blue shows Hoechst counterstaining. Scale bars, 20 μm. Error bars represent SEM. Also see Figure S5.

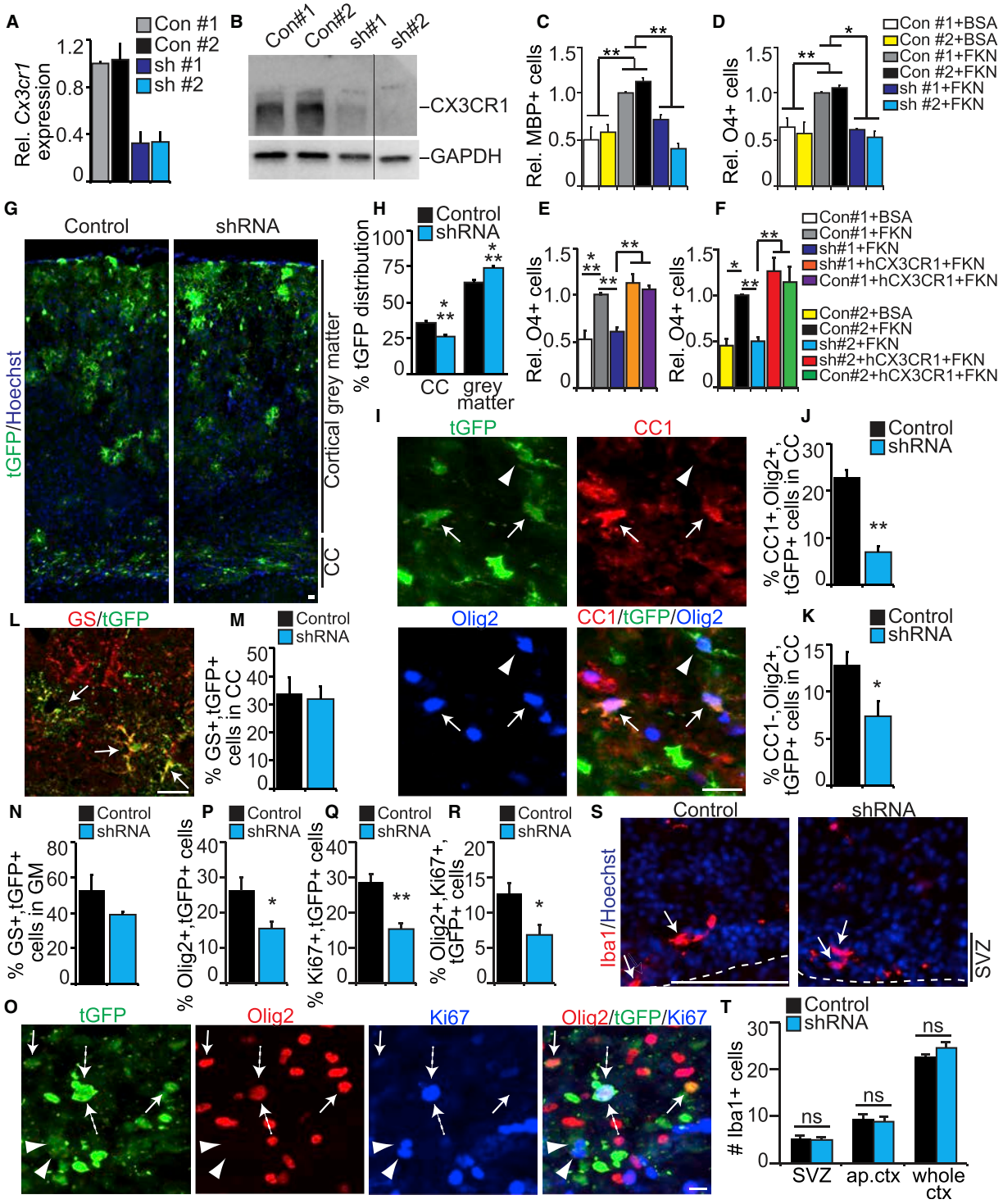

Figure 8. Fractalkine Signaling in Cortical Precursors Regulates Oligodendrogenesis

(A and B) HEK293 cells were co-transfected with a mouse CX3CR1 expression plasmid and a scrambled shRNA (Con #1), a luciferase shRNA (Con #2), or one of two murine CX3CR1 shRNAs (sh #1 and sh #2) and analyzed by qRT-PCR for mouse *Cx3cr1* mRNA (A) or western blots for CX3CR1 (B). In (A), data were

(legend continued on next page)

SUPPLEMENTAL INFORMATION

Supplemental Information includes six figures and three tables and can be found with this article online at http://dx.doi.org/10.1016/j.neuron.2017.04.018.

AUTHOR CONTRIBUTIONS

A.V. conceptualized, designed, performed, and analyzed most of the experiments and co-wrote the paper. S.A.Y. conceptualized, designed, and analyzed the transcriptome analysis and paracrine modeling and co-wrote the paper. B.S.W. worked with A.V. on a number of experimental analyses, and S.Z. contributed to FISH experiments. J.W. and C.S. performed the postnatal OPC culture experiments. D.R.K. conceptualized experiments and co-wrote the paper. F.D.M. conceptualized and designed experiments, analyzed data, and co-wrote the paper.

ACKNOWLEDGMENTS

This work was funded by grants to F.D.M. and D.R.K. from the CIHR (#329386), and to F.D.M., D.R.K., and J.W. from the Ontario Institute for Regenerative Medicine and the Canadian Stem Cell Network. F.D.M. and D.R.K. are Canada Research Chairs and F.D.M. is an HHMI Senior International Research Scholar. A.V. was funded by CIHR, MSSOC, and HSC Restracomp postdoctoral fellowships, S.A.Y. by an O.I.R.M. fellowship, and S.Z. by a CIHR MD/PhD studentship. We thank Sarah Burns, Matthew Seegobin, and Benigno Aquino for technical assistance.

Received: December 12, 2016
Revised: March 8, 2017
Accepted: April 12, 2017
Published: May 3, 2017

REFERENCES

Anderson, S.A., Eisenstat, D.D., Shi, L., and Rubenstein, J.L. (1997). Interneuron migration from basal forebrain to neocortex: dependence on Dlx genes. Science *278*, 474–476.

Barnabé-Heider, F., Wasylnka, J.A., Fernandes, K.J., Porsche, C., Sendtner, M., Kaplan, D.R., and Miller, F.D. (2005). Evidence that embryonic neurons regulate the onset of cortical gliogenesis via cardiotrophin-1. Neuron *48*, 253–265.

Binder, M.D., Cate, H.S., Prieto, A.L., Kemper, D., Butzkueven, H., Gresle, M.M., Cipriani, T., Jokubaitis, V.G., Carmeliet, P., and Kilpatrick, T.J. (2008). Gas6 deficiency increases oligodendrocyte loss and microglial activation in response to cuprizone-induced demyelination. J. Neurosci. *28*, 5195–5206.

Bustin, S.A., Benes, V., Garson, J.A., Hellemans, J., Huggett, J., Kubista, M., Mueller, R., Nolan, T., Pfaffl, M.W., Shipley, G.L., et al. (2009). The MIQE guidelines: minimum information for publication of quantitative real-time PCR experiments. Clin. Chem. *55*, 611–622.

Carvalho, B.S., and Irizarry, R.A. (2010). A framework for oligonucleotide microarray preprocessing. Bioinformatics *26*, 2363–2367.

Cook, A., Hippensteel, R., Shimizu, S., Nicolai, J., Fatatis, A., and Meucci, O. (2010). Interactions between chemokines: regulation of fractalkine/CX3CL1 homeostasis by SDF/CXCL12 in cortical neurons. J. Biol. Chem. *285*, 10563–10571.

Furuichi, K., Gao, J.L., and Murphy, P.M. (2006). Chemokine receptor CX3CR1 regulates renal interstitial fibrosis after ischemia-reperfusion injury. Am. J. Pathol. *169*, 372–387.

Gallagher, D., Voronova, A., Zander, M.A., Cancino, G.I., Bramall, A., Krause, M.P., Abad, C., Tekin, M., Neilsen, P.M., Callen, D.F., et al. (2015). Ankrd11 is a chromatin regulator involved in autism that is essential for neural development. Dev. Cell *32*, 31–42.

Garcia, J.A., Pino, P.A., Mizutani, M., Cardona, S.M., Charo, I.F., Ransohoff, R.M., Forsthuber, T.G., and Cardona, A.E. (2013). Regulation of adaptive immunity by the fractalkine receptor during autoimmune inflammation. J. Immunol. *191*, 1063–1072.

Gauthier-Fisher, A., and Miller, F.D. (2013). Environmental cues and signaling pathways that regulate neural precursor development. In Patterning and Cell Type Specification in the Developing CNS and PNS, J.L. Rubenstein and P. Rakic, eds. (Elsevier Press), pp. 355–383.

Gibson, E.M., Purger, D., Mount, C.W., Goldstein, A.K., Lin, G.L., Wood, L.S., Inema, I., Miller, S.E., Bieri, G., Zuchero, J.B., et al. (2014). Neuronal activity promotes oligodendrogenesis and adaptive myelination in the mammalian brain. Science *344*, 1252304.

Goudarzi, S., Rivera, A., Butt, A.M., and Hafizi, S. (2016). Gas6 promotes oligodendrogenesis and myelination in the adult central nervous system and after lysolecithin-induced demyelination. ASN Neuro *8*, 8.

normalized to *Gapdh* mRNA and expressed relative to the scrambled shRNA. In (B), the blot was probed for CX3CR1 and reprobed for GAPDH (lanes were spliced from the same autoradiogram as indicated by the vertical line).

(C and D) E13 cortical precursors were transfected with PB transposase and a scrambled shRNA (Con #1), an shRNA targeted to Luciferase (Con #2), or one of two murine CX3CR1 shRNAs (sh #1 and sh #2), all in a PB backbone that also encoded tGFP. Fractalkine (250 ng/mL) or vehicle (BSA) were added after 20 hr, and cultures were immunostained 7 days post-transfection for tGFP, MBP, and O4 (see Figure S6A). Graphs show the proportion of tGFP-positive cells that were also positive for MBP (C) or O4 (D), expressed relative to scrambled shRNA plus fractalkine. $^{**}p < 0.01$, $^{*}p < 0.05$; n = 3.

(E and F) E13 cortical precursors were transfected and cultured as in (C) and (D) except that some groups were also cotransfected with a human CX3CR1 expression plasmid. Graphs show the proportion of tGFP-positive cells that were also positive for O4, expressed relative to scrambled (E) or luciferase (F) shRNAs plus fractalkine. $^{*}p < 0.05$, $^{**}p < 0.01$, $^{***}p < 0.001$; n = 3.

(G–N) E14 cortices were electroporated with the PB transposase and CX3CR1 shRNA#2 (shRNA) or Luciferase shRNA (Control), both in a PB backbone that also encoded tGFP. Cortices were immunostained at P15 for tGFP (G, I, and L) and CC1 (red, I) plus Olig2 (blue, I), or for glutamine synthetase (GS, red, L), and the corpus callosum (CC) and cortical gray matter (GM) were quantified for the percentage of total tGFP-positive cells in the two regions (H), for tGFP-positive, Olig2-positive cells that did or did not express CC1 (J and K), or for tGFP-positive, glutamine synthetase-positive cells (M and N). Also See Figure S6B. In (G), sections were counterstained with Hoechst (blue). $^{*}p < 0.05$, $^{**}p < 0.01$, $^{***}p < 0.001$; n = 5 mice each. Arrows in (I) and (L) denote triple- or double-positive cells, respectively, while the arrowheads in (I) denote a tGFP-positive, CC1-negative, Olig2-positive OPC.

(O–R) Cortices were electroporated as in (G)–(N) and analyzed at P0 by immunostaining for tGFP (green, O), Olig2 (red, O), and Ki67 (blue, O). The apical cortex was then quantified for the percentage of tGFP-positive cells positive for Olig2 (P), Ki67 (Q), or both Olig2 and Ki67 (R). $^{*}p < 0.05$, $^{**}p < 0.01$; n = 4 mice each. In (O), hatched arrows denote a triple-positive cell, and arrows and arrowheads denote tGFP-positive cells that are positive only for Olig2 or Ki67, respectively.

(S and T) P0 cortical sections as in (O)–(R) were immunostained for Iba1 (red, arrows, S; also see Figure S6D), counterstained with Hoechst (blue, S), and the numbers of microglia in the SVZ, apical cortex (ap. ctx) and whole cortex (whole ctx) were quantified (T). ns, not significant; n = 4 mice each. Scale bars, 20 μm. Error bars represent SEM. Also see Figure S6.

Hadjantonakis, A.K., and Papaioannou, V.E. (2004). Dynamic in vivo imaging and cell tracking using a histone fluorescent protein fusion in mice. BMC Biotechnol. *4*, 33.

Ivanova, A., Nakahira, E., Kagawa, T., Oba, A., Wada, T., Takebayashi, H., Spassky, N., Levine, J., Zalc, B., and Ikenaka, K. (2003). Evidence for a second wave of oligodendrogenesis in the postnatal cerebral cortex of the mouse. J. Neurosci. Res. *73*, 581–592.

Johnston, A.P., Yuzwa, S.A., Carr, M.J., Mahmud, N., Storer, M.A., Krause, M.P., Jones, K., Paul, S., Kaplan, D.R., and Miller, F.D. (2016). Dedifferentiated schwann cell precursors secreting paracrine factors are required for regeneration of the mammalian digit tip. Cell Stem Cell *19*, 433–448.

Jung, S., Aliberti, J., Graemmel, P., Sunshine, M.J., Kreutzberg, G.W., Sher, A., and Littman, D.R. (2000). Analysis of fractalkine receptor CX(3)CR1 function by targeted deletion and green fluorescent protein reporter gene insertion. Mol. Cell. Biol. *20*, 4106–4114.

Kessaris, N., Fogarty, M., Iannarelli, P., Grist, M., Wegner, M., and Richardson, W.D. (2006). Competing waves of oligodendrocytes in the forebrain and postnatal elimination of an embryonic lineage. Nat. Neurosci. *9*, 173–179.

Lampron, A., Larochelle, A., Laflamme, N., Préfontaine, P., Plante, M.M., Sánchez, M.G., Yong, V.W., Stys, P.K., Tremblay, M.E., and Rivest, S. (2015). Inefficient clearance of myelin debris by microglia impairs remyelinating processes. J. Exp. Med. *212*, 481–495.

Ligon, K.L., Huillard, E., Mehta, S., Kesari, S., Liu, H., Alberta, J.A., Bachoo, R.M., Kane, M., Louis, D.N., Depinho, R.A., et al. (2007). Olig2-regulated lineage-restricted pathway controls replication competence in neural stem cells and malignant glioma. Neuron *53*, 503–517.

Limatola, C., and Ransohoff, R.M. (2014). Modulating neurotoxicity through CX3CL1/CX3CR1 signaling. Front. Cell. Neurosci. *8*, 229.

Livak, K.J., and Schmittgen, T.D. (2001). Analysis of relative gene expression data using real-time quantitative PCR and the 2(-Delta Delta C(T)) Method. Methods *25*, 402–408.

Lu, F., Chen, Y., Zhao, C., Wang, H., He, D., Xu, L., Wang, J., He, X., Deng, Y., Lu, E.E., et al. (2016). Olig2-dependent reciprocal shift in PDGF and EGF receptor signaling regulates tumor phenotype and mitotic growth in malignant glioma. Cancer Cell *29*, 669–683.

McKenzie, I.A., Ohayon, D., Li, H., de Faria, J.P., Emery, B., Tohyama, K., and Richardson, W.D. (2014). Motor skill learning requires active central myelination. Science *346*, 318–322.

Micheva, K.D., Wolman, D., Mensh, B.D., Pax, E., Buchanan, J., Smith, S.J., and Bock, D.D. (2016). A large fraction of neocortical myelin ensheathes axons of local inhibitory neurons. eLife *5*, 5.

Nadarajah, B., Alifragis, P., Wong, R.O., and Parnavelas, J.G. (2002). Ventricle-directed migration in the developing cerebral cortex. Nat. Neurosci. *5*, 218–224.

Nagy, K., Sung, H.K., Zhang, P., Laflamme, S., Vincent, P., Agha-Mohammadi, S., Woltjen, K., Monetti, C., Michael, I.P., Smith, L.C., and Nagy, A. (2011). Induced pluripotent stem cell lines derived from equine fibroblasts. Stem Cell Rev. *7*, 693–702.

O'Meara, R.W., Ryan, S.D., Colognato, H., and Kothary, R. (2011). Derivation of enriched oligodendrocyte cultures and oligodendrocyte/neuron myelinating co-cultures from post-natal murine tissues. J. Vis. Exp. (54), 3324.

Orduz, D., Maldonado, P.P., Balia, M., Vélez-Fort, M., de Sars, V., Yanagawa, Y., Emiliani, V., and Angulo, M.C. (2015). Interneurons and oligodendrocyte progenitors form a structured synaptic network in the developing neocortex. eLife *4*, 4.

Park, H.J., Baen, J.Y., Lee, Y.J., Choi, Y.H., and Kang, J.L. (2012). The TAM-family receptor Mer mediates production of HGF through the RhoA-dependent pathway in response to apoptotic cells. Mol. Biol. Cell *23*, 3254–3265.

Qiao, W., Wang, W., Laurenti, E., Turinsky, A.L., Wodak, S.J., Bader, G.D., Dick, J.E., and Zandstra, P.W. (2014). Intercellular network structure and regulatory motifs in the human hematopoietic system. Mol. Syst. Biol. *10*, 741.

Robinson, L.A., Nataraj, C., Thomas, D.W., Howell, D.N., Griffiths, R., Bautch, V., Patel, D.D., Feng, L., and Coffman, T.M. (2000). A role for fractalkine and its receptor (CX3CR1) in cardiac allograft rejection. J. Immunol. *165*, 6067–6072.

Ryan, T., Liu, J., Chu, A., Wang, L., Blais, A., and Skerjanc, I.S. (2012). Retinoic acid enhances skeletal myogenesis in human embryonic stem cells by expanding the premyogenic progenitor population. Stem Cell Rev. *8*, 482–493.

Sciumè, G., Soriani, A., Piccoli, M., Frati, L., Santoni, A., and Bernardini, G. (2010). CX3CR1/CX3CL1 axis negatively controls glioma cell invasion and is modulated by transforming growth factor-β1. Neuro-oncol. *12*, 701–710.

Shankar, S.L., O'Guin, K., Kim, M., Varnum, B., Lemke, G., Brosnan, C.F., and Shafit-Zagardo, B. (2006). Gas6/Axl signaling activates the phosphatidylinositol 3-kinase/Akt1 survival pathway to protect oligodendrocytes from tumor necrosis factor alpha-induced apoptosis. J. Neurosci. *26*, 5638–5648.

Sheridan, G.K., and Murphy, K.J. (2013). Neuron-glia crosstalk in health and disease: fractalkine and CX3CR1 take centre stage. Open Biol. *3*, 130181.

Srinivas, S., Watanabe, T., Lin, C.S., William, C.M., Tanabe, Y., Jessell, T.M., and Costantini, F. (2001). Cre reporter strains produced by targeted insertion of EYFP and ECFP into the ROSA26 locus. BMC Dev. Biol. *1*, 4.

Tsui, D., Voronova, A., Gallagher, D., Kaplan, D.R., Miller, F.D., and Wang, J. (2014). CBP regulates the differentiation of interneurons from ventral forebrain neural precursors during murine development. Dev. Biol. *385*, 230–241.

Venkatesh, H.S., Johung, T.B., Caretti, V., Noll, A., Tang, Y., Nagaraja, S., Gibson, E.M., Mount, C.W., Polepalli, J., Mitra, S.S., et al. (2015). Neuronal activity promotes glioma growth through Neuroligin-3 secretion. Cell *161*, 803–816.

Wu, S., Wu, Y., and Capecchi, M.R. (2006). Motoneurons and oligodendrocytes are sequentially generated from neural stem cells but do not appear to share common lineage-restricted progenitors in vivo. Development *133*, 581–590.

Xu, Q., Tam, M., and Anderson, S.A. (2008). Fate mapping Nkx2.1-lineage cells in the mouse telencephalon. J. Comp. Neurol. *506*, 16–29.

Yokota, Y., Gashghaei, H.T., Han, C., Watson, H., Campbell, K.J., and Anton, E.S. (2007). Radial glial dependent and independent dynamics of interneuronal migration in the developing cerebral cortex. PLoS ONE *2*, e794.

Yu, Y., Chen, Y., Kim, B., Wang, H., Zhao, C., He, X., Liu, L., Liu, W., Wu, L.M., Mao, M., et al. (2013). Olig2 targets chromatin remodelers to enhancers to initiate oligodendrocyte differentiation. Cell *152*, 248–261.

Yuzwa, S.A., Yang, G., Borrett, M.J., Clarke, G., Cancino, G.I., Zahr, S.K., Zandstra, P.W., Kaplan, D.R., and Miller, F.D. (2016). Proneurogenic ligands defined by modeling developing cortex growth factor communication networks. Neuron *91*, 988–1004.

Zhan, Y., Paolicelli, R.C., Sforazzini, F., Weinhard, L., Bolasco, G., Pagani, F., Vyssotski, A.L., Bifone, A., Gozzi, A., Ragozzino, D., and Gross, C.T. (2014). Deficient neuron-microglia signaling results in impaired functional brain connectivity and social behavior. Nat. Neurosci. *17*, 400–406.

Zhu, Y., Jin, K., Mao, X.O., and Greenberg, D.A. (2003). Vascular endothelial growth factor promotes proliferation of cortical neuron precursors by regulating E2F expression. FASEB J. *17*, 186–193.

STAR★METHODS

KEY RESOURCES TABLE

REAGENT or RESOURCE	SOURCE	IDENTIFIER
Antibodies		
chicken anti-eGFP	Abcam	Cat# ab13970; RRID: AB_300798
chicken anti-turbo GFP	Origene	Cat# TA150075
rabbit anti-turbo GFP	Thermo Fisher	Cat# PA5-22688; RRID: AB_2540616
rabbit anti-βIII-tubulin	Covance	Cat# 802001; clone# Poly18020; RRID: AB_2564645
mouse anti-βIII-tubulin	Covance	Cat# 801202; clone# TUJ1; RRID: AB_10063408
mouse anti-Ki67	BD PharMingen	Cat# 556003; RRID: AB_396287
rabbit anti-GFAP antibody	Dako	Cat# Z0334; RRID: AB_10013382
rat anti-MBP antibody	Millipore	Cat# MAB386; RRID: AB_94975
mouse IgM anti-O4	R&D Systems	Cat# MAB1326; RRID: AB_357617
rat anti-BrdU	ABD Serotec	Cat# OBT0030; RRID: AB_2313756
mouse anti-Nestin	Millipore	Cat# MAB5326; RRID: AB_11211837
rabbit anti-Olig2	Millipore	Cat# AB9610; RRID: AB_570666
mouse anti-Olig2	Millipore	Cat# MABN50; clone# Clone 211F1.1; RRID: AB_10807410
rabbit anti-PDGFRα	Santa Cruz	Cat# sc-338; RRID: AB_631064
mouse anti-GAD67	Millipore	Cat# MAB5406; RRID: AB_2278725
rat anti-SST	Millipore	Cat# MAB354; clone# YC7; RRID: AB_2255365
mouse anti-glutamine synthetase	Millipore	Cat# MAB302; clone# GS6; RRID: AB_2110656
goat anti-Sox2	Santa Cruz	Cat# sc-17320; RRID: AB_2286684
mouse anti-CC1	Calbiochem	Cat# OP80; RRID: AB_2057371
rabbit anti-Iba1	Wako	Cat# 019-19741; RRID: AB_839504
rabbit anti-cleaved CC3	Millipore	Cat# AB3623; RRID: AB_91556
rabbit anti-CX3CR1	Torrey Pines Biolabs	Cat# TP501; RRID: AB_10892355
rabbit anti-CX3CL1	Torrey Pines Biolabs	Cat# TP233; RRID: AB_10891146
mouse anti-GAPDH	Santa Cruz	Cat# sc-365062; RRID: AB_10847862
goat anti-Axl	R&D Systems	Cat# AF854; RRID: AB_355663
goat anti-Mertk	R&D Systems	Cat# AF591; RRID: AB_2098565
goat anti-Dtk/Tyro3	R&D Systems	Cat# AF759; RRID: AB_355579
Bacterial and Virus Strains		
Max Efficiency Stbl2 Competent Cells	Invitrogen	Cat# 10268-019
NEB 5-alpha Competent E.coli (High Efficiency)	NEB	Cat# C2987H
Biological Samples		
Embryonic and postnatal cortices and brains from CD1 and transgenic mice described in Experimental Models: Organisms and Strains below.	This paper	N/A
Chemicals, Peptides, and Recombinant Proteins		
Recombinant Mouse CX3CL1/Fractalkine Chemokine Domain	R&D Systems	Cat# 458-MF-025
Recombinant Mouse Gas6	R&D Systems	Cat# 986-GS
Recombinant Murine VEGF	Peprotech	Cat# 450-32
5-Bromo-2′-deoxyuridine (BrdU)	Sigma-Aldrich	Cat# B5002
Cytosineβ-D-arabinofuranoside	Sigma-Aldrich	Cat# C1768

(*Continued on next page*)

Continued

REAGENT or RESOURCE	SOURCE	IDENTIFIER
Critical Commercial Assays		
Mouse on Mouse (M.O.M.) Basic Kit	Vector Laboratories	Cat# BMK-2202
Mouse Gas6 ELISA kit	RayBiotech	Cat# ELM-GAS6
Mouse Fractalkine ELISA kit	RayBiotech	Cat# ELM-Fractalkine
Mouse VEGFA ELISA kit	RayBiotech	Cat# ELM-VEGF
RNAscope Fluorescent Multiplex Detection Reagents	ACDBio	Cat# 320851
E.Z.N.A. Total RNA Kit I	Omega BioTek	Cat# R6834
E.Z.N.A. MicroElute Total RNA Kit	Omega BioTek	Cat# R6831
SsoAdvanced Universal SYBR Green Supermix	Biorad	Cat# 1725271
QuantiTect Rev. Transcription Kit	QIAGEN	Cat# 205311
Deposited Data		
Raw microarray data from purified MGE interneurons	This paper	GEO: GSE95696
Ligands from microarray data from purified MGE interneurons	This paper	Table S1
Raw and analyzed microarray data from embryonic cortical precursors	Yuzwa et al., 2016	GEO: GSE84482
Experimental Models: Cell Lines		
Human: HEK293 cell line, Female Sex	ATCC	Cat# PTA-4488; RRID: CVCL_0045
Experimental Models: Organisms/Strains		
H2BBGFP (B6.Cg-Tg(HIST1H2BB/EGFP)1Pa/J)	The Jackson Laboratory	Cat# JAX:006069; RRID: IMSR_JAX:006069
Nkx2.1Cre (C57BL/6J-Tg(Nkx2-1-cre)2Sand/J)	The Jackson Laboratory	Cat# JAX:008661; RRID: IMSR_JAX:008661
DTA^{stop} (B6;129-Gt(ROSA)26$Sor^{tm1(DTA)Mrc}$/J)	The Jackson Laboratory	Cat# JAX:010527; RRID: IMSR_JAX:010527
YFP^{stop} (B6.129X1-Gt(ROSA)26$Sor^{tm1(EYFP)Cos}$/J)	The Jackson Laboratory	Cat# JAX:006148; RRID: IMSR_JAX:006148
$CX3CR1^{-/-}$ (B6.129P-Cx3cr1^{tm1Litt}/J)	The Jackson Laboratory	Cat# JAX:005582; RRID:I MSR_JAX:005582
CD1	Charles River	Cat# 022
Oligonucleotides		
For shRNA sequences, please see Table S2	This paper	N/A
For genotyping primer sequences, please see Table S3	The Jackson Laboratory	N/A
qPCR *Fkn*-specific primer sequence, forward: ACGAAATGCGAAATCATGTGC	Primer Bank	Primer Bank ID# 31982017a1
qPCR *Fkn*-specific primer sequence, reverse: CTGTGTCGTCTCCAGGACAA	Primer Bank	Primer Bank ID# 31982017a1
qPCR *Cx3cr1*-specific primer sequence, forward: CGGCCATCTTAGTGGCGTC	Primer Bank	Primer Bank ID# 87299631c3
qPCR *Cx3cr1*-specific primer sequence, reverse: GGATGTTGACTTCCGAGTTGC	Primer Bank	Primer Bank ID# 87299631c3
qPCR mouse *Gapdh*-specific primer sequence, forward: GGGTGTGAACCACGAGAAATA	Gallagher et al., 2015	N/A
qPCR mouse *Gapdh*-specific primer sequence, reverse: CTGTGGTCATGAGCCCTTC	Gallagher et al., 2015	N/A
qPCR human *Gapdh*-specific primer sequence, forward: TGGTGCTGAGTATGTCGTGGAGT	Ryan et al., 2012	N/A
qPCR human *Gapdh*-specific primer sequence, reverse: AGTCTTCTGAGTGGCAGTGATGG	Ryan et al., 2012	N/A
Recombinant DNA		
PiggyBac eGFP (PCAG-PB-EGFP) and *piggybac* Transposase plasmids (PCAG-PBase)	Nagy et al., 2011	Nagy et al., 2011
PiggyBac tGFP and *super piggybac* Transposase plasmids	SBI	Cat# PBSI506A-1 and PB210PA-1

(*Continued on next page*)

Continued

REAGENT or RESOURCE	SOURCE	IDENTIFIER
Mouse CX3CR1 plasmid	IMAGE consortium, Centre for Applied Genomics at the Hospital for Sick Children	IMAGE clone IMAGE: 4017224 (IRAV22C12)
Human CX3CR1 plasmid	IMAGE consortium, Centre for Applied Genomics at the Hospital for Sick Children	IMAGE clone IMAGE: 5216452 (IRAT49B6)
Software and Algorithms		
Robust Multichip Analysis (RMA) algorithm using the Oligo bioconductor package in R	Carvalho and Irizarry, 2010; http://bioconductor.org/packages/release/bioc/html/oligo.html	http://bioconductor.org/packages/release/bioc/html/oligo.html
Python (version 2.7.6)	http://www.python.org/	RRID: SCR_008394
Paracrine interaction module algorithm	Johnston et al., 2016	N/A
Prism 5	GraphPad	https://www.graphpad.com/scientific-software/prism/; RRID: SCR_002798
Volocity software	Improvision	http://www.perkinelmer.com/lab-solutions/resources/docs/BRO_VolocityBrochure_PerkinElmer.pdf; RRID: SCR_002668
ZEN software	Zeiss Microscope	https://www.zeiss.com/microscopy/int/products/microscope-software/zen.html; RRID: SCR_013672
Adobe Illustrator CC	Adobe	http://www.adobe.com/products/illustrator.html; RRID: SCR_010279
Adobe Photoshop CC	Adobe	https://www.adobe.com/products/photoshop.html; RRID: SCR_014199
Other		
FISH probe: Mouse *Cx3cl1* (*Fkn*) (GenBank: NM_009142.3), channel 1	ACDBio	Cat# 426211
FISH probe: Mouse *Cx3cr1* (GenBank: NM_009987.4), channel 2	ACDBio	Cat# 314221-C2
FISH probe: Mouse *Olig2* (GenBank: NM_016967.2), channel 1	ACDBio	Cat# 447091
FISH probe: Mouse *Pdgfrα* (GenBank: NM_011058.2), channel 1	ACDBio	Cat# 480661
FISH probe: Mouse *Sox2* (GenBank: NM_011443.3), channel 3	ACDBio	Cat# 401041-C3
FISH probe: Mouse *Sst* (GenBank: NM_009215.1), channel 2	ACDBio	Cat# 404631-C2

CONTACT FOR REAGENT AND RESOURCE SHARING

Further information and requests for resources and reagents should be directed to and will be fulfilled by the Lead Contact, Freda Miller (fredam@sickkids.ca).

EXPERIMENTAL MODEL AND SUBJECT DETAILS

Mice

All animal use was approved by the Animal Care Committee of the Hospital for Sick Children in accordance with the Canadian Council of Animal Care policies. Mice were maintained on a 12 hr light/dark cycle, and food and water was provided ad libitum. All mice were healthy with no obvious behavioral phenotypes, and none of the experimental mice were immune compromised. For all mouse studies, mice of either sex were used and mice were randomly allocated to experimental groups. Developmental ages between embryonic day (E) 12 - postnatal day (P) 15 were used. Specific end-point developmental ages used for each experiment are indicated in the figure legends. CD1 mice, purchased from Charles River Laboratory, were used for culture and in utero electroporation

experiments unless indicated otherwise. H2BBGFP (B6.Cg-Tg(HIST1H2BB/EGFP)1Pa/J, RRID:IMSR_JAX:006069) (Hadjantonakis and Papaioannou, 2004), Nkx2.1Cre (C57BL/6J-Tg(Nkx2-1-cre)2Sand/J, RRID: IMSR_JAX:008661) (Xu et al., 2008), DTA^{stop} (B6;129-Gt(ROSA)26$Sor^{tm1(DTA)Mrc}$/J, RRID: IMSR_JAX:010527) (Wu et al., 2006), YFP^{stop} (B6.129X1-Gt(ROSA)26$Sor^{tm1(EYFP)Cos}$/J, RRID: IMSR_JAX:006148) (Srinivas et al., 2001), $CX3CR1^{-/-}$ (B6.129P-Cx3cr1^{tm1Litt}/J, RRID: IMSR_JAX:005582) (Jung et al., 2000) and wild-type (WT) C57BL/6J mice were obtained from Jackson Laboratories. For genetic ablation experiments, Nkx2.1Cre-positive females were bred with DTA^{stop}-positive heterozygous males. In some experiments, Nkx2.1Cre-positive females that were bred with DTA^{stop}-positive heterozygous males were used for in utero electroporation or were injected with 100 mg/kg BrdU at E18.5 and newborn pups were analyzed the next day. For lineage tracing experiments, Nkx2.1Cre-positive mice were bred with YFP^{stop}-positive mice. H2BBGFP-positive mice were bred to WT C57BL/6J mice and the resulting H2BBGFP-positive E13 embryos were used for purification of MGE interneurons as described below. $CX3CR1^{-/-}$ mice were bred to WT C57BL/6J mice to obtain $CX3CR1^{+/-}$ progeny. $CX3CR1^{+/-}$ mice were then bred to obtain $CX3CR1^{+/+}$, $CX3CR1^{+/-}$ and $CX3CR1^{-/-}$ pups that were used for analysis. All mice were bred and genotyped as recommended by Jackson Laboratories. The genotyping primers are in Table S3.

HEK293 cell cultures and transfections

HEK293 cells were maintained in DMEM (GIBCO) supplemented with 10% fetal bovine serum (FBS) and 1% penicillin-streptomycin. For transfection experiments, 200,000 cells were seeded in 6-well tissue culture dishes and 48h later transfected with Lipofectamine 3000 (Invitrogen) and 2 μg total plasmid DNA according to manufacturer's instructions. For shRNA validation experiments, cells were transfected with 1 μg of mouse CX3CR1 expression plasmid and 1 μg of *Super PiggyBac* plasmid encoding turbo-GFP and scrambled shRNA or shRNA against Luciferase or CX3CR1 described below. 8h after transfection, the medium was changed and 48h after transfection, cells were collected for qRT-PCR and western blot analysis.

MGE interneuron cultures

E13 MGE tissue was dissected from pooled CD1 or H2BBGFP-positive embryos of either sex from the same mother and cultured as described (Tsui et al., 2014). Briefly, embryos were maintained on ice in Hank's balanced salt solution (HBSS, GIBCO) during dissection. Following removal of the cortex and meninges to expose the ventral forebrain, MGE tissue was excised and mechanically triturated in Neurobasal medium (GIBCO) containing 40 ng/ml FGF2 (BD Biosciences), 2% B27 supplement (GIBCO), and 500 μM L-Glutamine (GIBCO). Triturated MGE cells were plated on to four-well chamber slides (Nunc), 6-well tissue culture plates (Falcon) or microscope cover glass slips (Fisher) pre-coated with 2% laminin (BD Biosciences) and 1% poly-D-lysine (Sigma) at a density of 59,000 cells/cm^2. On day 5 of culture, 1 μM cytosine β arabinofuranoside C (AraC, Sigma) was added. After 24h of AraC treatment, the medium was changed 3 times at 2h intervals to wash out the AraC and dead cells. Purified MGE neurons were then cultured for 2 additional days to condition fresh medium or were used for co-culture experiments.

Conditioned medium preparation

MGE interneurons were purified as described above and cultured on 6-well tissue culture plates (Falcon) pre-coated with 2% laminin (BD Biosciences) and 1% poly-D-lysine (Sigma). After AraC treatment and wash-out, purified MGE interneurons were cultured in Neurobasal medium supplemented with 40 ng/ml FGF2, 2% B27 supplement, and 500 μM L-Glutamine for 42-44h. This conditioned medium was then collected, and any floating cells were removed by centrifugation at 1,000 g for 5 min. Supernatant was collected and re-supplemented with 40 ng/ml FGF2, 2% B27 supplement, 1% Penicillin and Streptomycin (Lonza) and 500 μM L-Glutamine. Conditioned medium was used immediately for cortical precursor culture experiments. Control Neurobasal medium supplemented with 40 ng/ml FGF2, 2% B27 supplement, and 500 μM L-Glutamine was added to sterile 6-well tissue culture plates (Falcon) pre-coated with 2% laminin (BD Biosciences) and 1% poly-D-lysine (Sigma) without any cells and was incubated in a separate dish at the same time as conditioned medium. Control medium was collected, centrifuged and re-supplemented as described above for the conditioned medium.

Cortical precursor cell culture and transfections

Cortices were dissected from pooled E13 CD1 embryos of either sex from the same mother and cultured as described (Yuzwa et al., 2016). Briefly, meninges were removed and the exposed neocortex was collected and mechanically triturated as for the MGE tissue, described above. Cortical cells were then plated onto four- or eight-well chamber slides (Nunc) or microscope cover glass slips (Fisher) pre-coated with 2% laminin (BD Biosciences) and 1% poly-D-lysine (Sigma) at a density of 59,000 cells/cm^2. Cells were cultured in Neurobasal medium (GIBCO) containing 40 ng/ml FGF2 (BD Biosciences), 2% B27 supplement (GIBCO), 1% Penicillin and Streptomycin (Lonza), and 500 μM L-Glutamine (GIBCO). For transfections, cortical cultures were transfected with Lipofectamine LTX with PLUS (Fisher) and 1 μg total plasmid DNA according to the manufacturer's instructions. For clonal analysis, 0.5 μg of *PiggyBac* eGFP and 0.5 μg of *PiggyBac* transposase expression plasmids were used. For knockdown experiments, 0.5 μg of *Super PiggyBac* plasmid encoding turbo-GFP and scrambled shRNA or shRNA against Luciferase or CX3CR1, and 0.5 μg of *Super PiggyBac* transposase expression plasmid were used. For rescue experiments, 0.33 μg of *Super PiggyBac* plasmid encoding turbo-GFP and scrambled shRNA or shRNA against Luciferase or CX3CR1, 0.33 μg of *Super PiggyBac* transposase expression plasmid, and 0.33 μg of human CX3CR1 expression plasmids were used. 16h after transfection, half of the medium was changed. In some experiments, fractalkine (FKN, R&D Systems) was added at 250 ng/ml concentration. For growth factor analysis, Gas6

(R&D Systems) was added to culture at 50, 100 and 250 ng/ml, VEGFA (Peprotech) at 10, 50 and 100 ng/ml, or fractalkine (FKN, R&D Systems) at 100, 250 and 500 ng/ml. BSA dissolved in PBS was used as the vehicle control. In some experiments, function-blocking antibodies (described in detail below) were added at 20 μg/ml or, for anti-CX3CR1, at 40 μg/ml. Goat or rabbit non-specific IgG were used as isotype controls. For BrdU assays, BrdU (Sigma) was added to cultures at 3 μg/ml for 24h.

Co-culture experiments

MGE interneurons were purified from E13 H2BBGFP-positive embryos as described above using four-well chamber slides (Nunc). After AraC treatment and wash-out, MGE interneurons were allowed to recover for 24 - 40 hr. Freshly dissected cortical precursors from wild-type E13 CD1 embryos were then added to the MGE interneurons at densities of 59,000 cells/cm^2 or 29,500 cells/cm^2 for analysis 2 or 7 days later, respectively. As a control, cortical precursors were added to similar sterile pre-coated wells with no prior cultured cells at comparable densities. Half of the medium was then changed every other day.

Postnatal OPC cultures

Meninges were removed from the cortex of P0 C57BL/6 mice of either sex and mixed glial cultures from cortices were prepared as described (O'Meara et al., 2011). Oligodendroglial precursor cells were enriched from these mixed glial cultures by shaking as described in O'Meara et al. (2011). The resultant cultures were comprised of, on average, 50% Olig2-positive oligodendroglial precursors. For proliferation and differentiation assays, cells were seeded at 12,500 cells/cm^2 onto 1 mg/mL Poly-L-lysine- and 10 μg/mL laminin-coated coverslips. For proliferation assays, plated cells were cultured in proliferation medium containing 10% Fetal Bovine Serum (FBS, GIBCO), 1% Glutamax (Invitrogen), 5 μg/ml bovine insulin (Sigma), 0.33% Penicillin and Streptomycin (Lonza) and 4.5 g/L D-glucose in DMEM medium (Multicell). BrdU (3 μg/ml; Sigma) was added on day 2 and cultures were analyzed 16 hr later. For differentiation assays, plated cells were cultured for 4 days in differentiation medium containing 5 μg/mL bovine insulin (Sigma), 0.01 mg/ml BSA (Sigma), 0.06 μg/ml progesterone (Sigma), 0.016 mg/ml putrescine (Sigma), 0.005 μg/ml sodium selenite (Sigma), 0.4 μg/ml 3,3′,5-Triiodo-L-thyronine (Sigma), 2% B27 (GIBCO), 50 ng/mL CNTF (Peprotech), 1% Glutamax (Invitrogen), 50 μg/mL Holotransferin (Sigma), 0.5% FBS, 0.33% Penicillin and Streptomycin (Lonza) and 4.5 g/L D-glucose in DMEM medium.

METHOD DETAILS

All culture and animal experiments were quantified blinded as to the experimental manipulation. Mice were randomly allocated to experimental groups and all data collected in the course of these studies were included in the individual analyses. No data were excluded and therefore there were no exclusion criteria. Due to technical limitations on sample collection no sample-size estimates were conducted. All attempts were made to use a maximal sample size in each experiment whenever possible.

Plasmids

PiggyBac eGFP and *PiggyBac* transposase expression plasmids are described elsewhere (Nagy et al., 2011). The *Super PiggyBac* shRNA vector encoding turbo-GFP under control of the EF1α promoter was purchased from SBI Biosciences. Two plasmids encoding short-hairpin sequences targeting different regions of mouse CX3CR1 mRNA (GenBank: NM_009987.4, 596-616 nt or 1104-1124 nt) were generated by annealing the following oligonucleotides: 5′- GATCGTTCATGTTCACAAAGAGAAATTCAAGAGATTTCTCTTTGTGAACATGAACTTTTT-3′ and 5′- AATTAAAAAGTTCATGTTCACAAAGAGAAATCTCTTGAATTTCTCTTTGTGAACATGAAC-3′ or 5′- GATCGACAGCATTCTGAGCAGTTTCTTCAAGAGAGAAACTGCTCAGAATGCTGTCTTTTT-3′ and 5′- AATTAAAAAGACAGCATTCTGAGCAGTTTCTCTCTTGAAGAAACTGCTCAGAATGCTGTC-3′ (CX3CR1-targeting sequences are underlined). The annealed oligos were inserted into *Super PiggyBac* shRNA vector via EcoRI and BamHI restriction sites. One scrambled control was generated by annealing the following oligonucleotides: 5′- GATCACAAGATGAAGAGCACCAATTCAAGAGATTGGTGCTCTTCATCTTGTTGTTTTT-3′ and 5′- AATTAAAAACAACAAGATGAAGAGCACCAATCTCTTGAATTGGTGCTCTTCATCTTGT-3′. Another control shRNA against Luciferase was generated by annealing the following oligonucleotides: 5′- GATCGGATTTCAGTCGATGTACATTCAAGAGATGTACATCGACTGAAATCCTTTTT-3′ and 5′- AATTAAAAAGGATTTCAGTCGATGTACATCTCTTGAATGTACATCGACTGAAATCC-3′. Scrambled and Luciferase-targeting sequences are underlined. The DNA sequence encoding the *Supper PiggyBac* transposase from *Supper PiggyBac* transposase expression plasmid (SBI) was inserted into the PUC19 vector (NEB) using SmaI and HindIII restriction sites. Expression plasmids for mouse and human CX3CR1 encompassing both cDNA and UTR sequences in pCMV-SPORT6 vectors were obtained from IMAGE cDNA clones from the Centre for Applied Genomics at the Hospital for Sick Children: mouse CX3CR1 IMAGE clone #4017224 (IRAV22C12) and human CX3CR1 IMAGE clone #5216452 (IRAT49B6). All plasmids were verified by appropriate restriction digest and sequencing.

Growth factors and function-blocking antibodies

Murine Gas6 and fractalkine were obtained from R&D Systems, and murine VEGFA from Peprotech. All growth factors were reconstituted in 0.1% bovine serum albumin (BSA) in sterile phosphate-buffered saline (PBS). Gas6 was reconstituted at 50 μg/ml, and fractalkine and VEGFA were reconstituted at 100 μg/ml. Function-blocking antibodies specific for murine Gas6 receptors Axl (AF854, RRID: AB_355663), Mertk (AF591, RRID: AB_2098565) and Dtk/Tyro3 (AF759, RRID: AB_355579) were obtained from R&D Systems. Function-blocking antibodies specific for murine fractalkine ligand (FKN, TP233, RRID: AB_10891146) and rat

fractalkine receptor CX3CR1 (TP501, RRID: AB_10892355) were obtained from Torrey Pines Biolabs. Goat and rabbit non-specific IgGs were obtained from Millipore. These function-blocking antibodies have been previously characterized elsewhere (Furuichi et al., 2006; Park et al., 2012; Robinson et al., 2000).

Lineage tracing experiments

Nkx2.1Cre-positive mice were bred with YFP^{stop}-positive mice. Nkx2.1Cre-positive, YFP^{stop}-positive embryos at E15.5 or pups at postnatal day 0 (P0) were harvested, brains dissected and fixed in 4% paraformaldehyde (PFA) for 24 hr. Brains were then cryopreserved in 30% sucrose for 48 hr, mounted in O.C.T compound (Tissue-Tek) and cryosectioned coronally to produce 16 μm sections.

Genetic ablation experiments

Nkx2.1Cre-positive females were mated with DTA^{stop}-positive heterozygous males to produce Nkx2.1Cre-negative, DTA^{stop}-positive (Cre-DTA+), Nkx2.1Cre-positive, DTA^{stop}-negative (Cre+DTA-) and Nkx2.1Cre-positive, DTA^{stop}-positive (Cre+DTA+) mice that were collected at birth (postnatal day P0) or at E18.5. For some experiments, pregnant mothers were injected with 100 mg/kg BrdU at E18.5 and analyzed the next day (P0). For analysis at E18.5, embryos were in utero electroporated with *PiggyBac* eGFP and *PiggyBac* transposase expression plasmids to label the progeny of cortical precursors, as described below.

In utero electroporations

CD1 pregnant mothers, or pregnant Nkx2.1Cre-positive mothers mated with DTA^{stop}-positive heterozygous males, were used for in utero electroporations at gestational day 14 (E14) as described (Gallagher et al., 2015; Yuzwa et al., 2016). For CD1 mice, 0.75 μg of *Super PiggyBac* plasmid encoding turbo-GFP and shRNA against Luciferase (Control) or shRNA against CX3CR1 (shRNA #2), and 0.75 μg of *Super PiggyBac* transposase expression plasmid were used for every embryo. 0.5% Trypan Blue was used as a visual tracer. To distinguish between control and shCX3CR1 electroporated cortices from the same litter, control plasmid was injected into left lateral ventricle, and shCX3CR1 plasmid was injected into right lateral ventricle. A CUY21 EDIT (TR Tech, Japan) electroporator was used to deliver five 50 ms pulses of 40-50 V with 950 ms intervals per embryo. At birth (postnatal day P0) or at postnatal day 15 (P15), pups were collected and brains were dissected and fixed in 4% paraformaldehyde (PFA) for 24 hr. Brains were then cryopreserved in 30% sucrose for 48-72 hr, mounted in O.C.T compound (Tissue-Tek) and cryosectioned coronally to produce 16-18 μm sections. For pregnant Nkx2.1Cre-positive mothers mated with DTA^{stop}-positive heterozygous males, 0.75 μg of *PiggyBac* eGFP and 0.75 μg of *PiggyBac* transposase expression plasmids were used for electroporation of each embryo as described above. Embryos were collected at E18.5 and brains were dissected, cryopreserved and sectioned as described above.

Immunostaining

For immunostaining of cells, cultures were fixed with 4% PFA for 10 min at room temperature, permeabilized with 0.2% NP-40 (USB) in PBS and blocked with 0.5% BSA and 6% normal donkey serum (Jackson ImmunoResearch) in PBS for 1h at room temperature. Cultures were then incubated with primary antibodies at 4°C overnight followed by appropriate fluorescently labeled secondary antibodies (1:1,000) for 1h at room temperature. For BrdU immunostaining, after incubation with the fluorescently labeled secondary antibodies, sections were washed 3 times with PBS, post-fixed in 4% PFA for 10 min at room temperature, washed again with PBS, and were incubated with 1M hydrochloric acid (HCl) for 10 min at 4°C and 2M HCl for 20 min at room temperature. After extensive washes with PBS, slides were blocked with 5% normal donkey serum (Jackson ImmunoResearch), 0.3% Triton X-100 and 1M glycine (BioBasic), incubated with anti-BrdU (rat, ABD Serotec) diluted in PBS (1:300) at 4°C overnight and then with a fluorophore-conjugated anti-rat secondary antibody for 1h at room temperature. For visualization of nuclei, cultures were counterstained with Hoechst 33258 for 2 min. Slides were mounted using Permafluor mounting media (Thermo Fisher).

For immunostaining of tissue sections, the sections were rehydrated in PBS for 10 min at room temperature and blocked using 5% BSA (Jackson ImmunoResearch) and 0.3% Triton X-100 (Fisher) in PBS for 1h at room temperature. Tissue sections were then incubated with appropriate primary antibodies diluted in 5% BSA in PBS. For primary antibodies raised in mouse, an MOM (mouse-on-mouse) kit was used according to the manufacturer's protocol (Vector Laboratories). Appropriate fluorescently labeled secondary antibodies (1:1,000) were used for 1h at room temperature. For visualization of nuclei, sections were counterstained with Hoechst 33258 for 2 min. Slides were mounted using Permafluor mounting media (Thermo Fisher). For BrdU staining, after incubation with the fluorescently labeled secondary antibodies, sections were washed 3 times with PBS, post-fixed in 4% PFA for 10 min at room temperature, washed again with PBS, and were incubated with 1M hydrochloric acid (HCl) for 10 min at 4°C and 2M HCl for 10 min at room temperature and then 20 min at 37°C. After extensive washes with PBS, slides were blocked with 5% normal donkey serum (Jackson ImmunoResearch), 0.3% Triton X-100 and 1M glycine (BioBasic), incubated with anti-BrdU (rat, ABD Serotec) diluted in PBS (1:300) at 4°C overnight and then with Cy5-conjugated anti-rat secondary antibody for 1h at room temperature. Sections were counterstained with Hoechst 33258 for 2 min and then mounted using Permafluor mounting media (Thermo Fisher).

Antibodies

The following primary antibodies were used in this study: chicken anti-eGFP (Abcam, 1:1,000, immunostaining, RRID: AB_300798), chicken anti-turbo GFP (Origene, 1:1,000, immunostaining), rabbit anti-turbo GFP (Thermo Fisher, 1:2,000, immunostaining, RRID: AB_2540616), rabbit anti-βIII-tubulin (Covance, 1:2,000, immunostaining, RRID: AB_10063850), mouse anti-βIII-tubulin (Covance,

1:1,000, immunostaining, RRID: AB_2313773), mouse anti-Ki67 (BD PharMingen, 1:300, immunostaining, RRID: AB_396287), rabbit anti-GFAP antibody (Dako, 1:400, immunostaining, RRID: AB_10013382), rat anti-MBP antibody (Millipore 1:300, immunostaining, RRID: AB_94975), mouse IgM anti-O4 (Millipore, 1:1,000, immunostaining, RRID: AB_357617), rat anti-BrdU (ABD Serotec, 1:300, immunostaining, RRID: AB_2313756), mouse anti-Nestin (Millipore, 1:500, immunostaining, RRID: AB_11211837), rabbit anti-Olig2 (Millipore, 1:1,000, immunostaining, RRID: AB_570666), mouse anti-Olig2 (Millipore, 1:1,000, immunostaining, RRID: AB_10807410), rabbit anti-PDGFRα (Santa Cruz, 1:300, immunostaining, RRID: AB_631064), mouse anti-GAD67 (Millipore, 1:200, immunostaining, RRID: AB_2278725), rat anti-SST (Millipore, 1:200, immunostaining, RRID: AB_2255365), mouse anti-glutamine synthetase (Millipore, 1:200, immunostaining, RRID: AB_2110656), goat anti-Sox2 (Santa Cruz, 1:500, immunostaining, RRID: AB_2286684), rabbit anti-Sox2 (Cell Signaling, 1:500, immunostaining, RRID: AB_2194037), mouse anti-CC1 (Calbiochem, 1:200, immunostaining, RRID: AB_2057371), rabbit anti-Iba1 (Wako, 1:1,000, immunostaining, RRID: AB_839504), rabbit anti-cleaved CC3 (Millipore, 1:500, immunostaining, RRID: AB_91556), rabbit anti-CX3CR1 (Torrey Pines Biolabs, 1:2,000, for detection of over-expressed mouse CX3CR1, western blot, RRID: AB_10892355), mouse anti-GAPDH (Santa Cruz, 1:5,000, western blot, RRID: AB_10847862). Fluorescently labeled highly cross-absorbed secondary antibodies were purchased from Jackson ImmunoResearch and used at 1:1,000 dilution. If the MOM kit was used, Cy3-, DTAF-, or Cy5-conjugated streptavidin (Jackson ImmunoResearch) were used at 1:1,000 dilution. For western blot application, horseradish peroxidase (HRP)-conjugated anti-mouse or anti-rabbit secondary antibodies (GE Healthcare) were used at 1:1,000 dilution.

Fluorescent in situ hybridization (FISH)

The single molecule FISH was performed as described in (Yuzwa et al., 2016) with probes targeting *Fkn* (GenBank: NM_009142.3), *Cx3cr1* (GenBank: NM_009987.4), *Olig2* (GenBank: NM_016967.2), *Pdgfrα* (GenBank: NM_011058.2), *Sox2* (GenBank: NM_011443.3) and *Sst* (GenBank: NM_009215.1) mRNA by using the RNAscope kit (Advanced Cell Diagnostics) according to the manufacturer's instructions. Briefly, freshly dissected brains of E15.5 and E17.5 CD1 embryos and P0, P3 and P4 CD1 pups, or E18.5 brains from Nkx2.1Cre-negative, DTA^{stop}-positive (Cre-DTA+), Nkx2.1Cre-positive, DTA^{stop}-negative (Cre+DTA-) and Nkx2.1Cre-positive, DTA^{stop}-positive (Cre+DTA+) embryos electroporated at E14 with PB-eGFP and PB transposase, were fixed in 4% PFA overnight and cryopreserved in 30% sucrose for 24h. Brains were snap-frozen in O.C.T. and sectioned coronally at 16 μm thickness. E13 MGE and cortical precursor cells or purified MGE neurons were cultured on microscope cover glass slips (Fisher) pre-coated with 2% laminin (BD Biosciences) and 1% poly-D-lysine (Sigma) as described above. Cell cultures were fixed with 4% PFA for 15 min. Fixed sections or cell cultures were washed with ethanol, followed by tissue pretreatment, probe hybridization and signal amplification. For purified MGE interneuron cultures, cells were immunostained with a Gad67-specific antibody following FISH. Sections and cells were counterstained with DAPI to visualize nuclei. Positive FISH signals were identified as punctate dots present in the nucleus and/or cytoplasm. Z stacks of confocal images were taken with optical slice thickness 0.2 μm and stacked images are shown.

Western blotting

HEK293 cells transfected with mouse CX3CR1 expression plasmid and plasmids encoding scrambled shRNA, shRNA against Luciferase, or mouse CX3CR1 were cultured for 48h and lysed in radioimmunoprecipitation (RIPA) buffer containing 50 mM Tris, pH7.4, 150 mM NaCl, 1% NP-40, 0.25% Na-deoxycholate, 1 mM EDTA, 1x protease inhibitor cocktail (Roche) and 0.5 mM phenylmethanesulfonylfluoride (PMSF) (Sigma-Aldrich). Lysates were clarified by centrifugation for 15 min at 13000 g. 40 μg of total protein was resolved using 4%–15% gradient mini-PROTEAN TGX gels (Biorad) according to the manufacturer's protocol. Resolved proteins were transferred to polyvinylidene fluoride (PVDF) membrane, blocked in 5% BSA (GE Healthcare), and incubated with CX3CR1- and GAPDH-specific antibodies. Signal was detected using Horseradish Peroxidase (HRP)-conjugated secondary anti-rabbit or anti-mouse (GE Healthcare), followed by a chemiluminescence reaction using Amersham ECL substrate (GE Healthcare). Chemiluminescent signal was detected using the MicroChemi4.2 system (DNR Bioimaging Systems).

Microarray and qRT-PCR

Total RNA was isolated from MGE interneurons purified as above, from dissected cortices of E12.5, E13.5, E15.5, E17.5, P0, P4 and P15 CD-1 embryos or pups, or from HEK293 cells using the E.Z.N.A. Total RNA or MicroElute Total RNA kits (Omega Biotek). For microarray analysis, DNA was digested on-column during RNA purification using DNase I (Omega Biotek). For microarray analysis, RNA was independently isolated from MGE interneurons cultured from embryos of 3 different CD-1 mothers and analyzed at the Center for Applied Genomics at the Hospital for Sick Children. RNA quality was confirmed using the Bioanalyzer. cDNA was generated using 100 ng of total RNA and Ambion Whole Transcriptome (WT) kit (Applied Biosystems). 5.5 ug of labeled cDNA was hybridized onto Mouse Gene 2.0 ST arrays using the Affymetrix FS450_0002 hybridization protocol, and scanned using the Affymetrix GeneChip Scanner 3000. For quantitative real-time PCR (qRT-PCR) analysis, cDNA was generated using 250 ng – 1 μg of total RNA and the Quantitect Reverse Transcription Kit (QIAGEN) according to manufacturer's instructions. 1/40th of the RT reaction was used as a template for qRT-PCR amplification using specific primers listed below and the FastStart SYBR Green kit (Roche) or SsoAdvanced Universal SYBR Green Mastermix (Biorad). Data was acquired using CFX96 or CFX384 instruments (Biorad). Data was normalized to GAPDH and quantified using the $2^{-\Delta\Delta Ct}$ method (Livak and Schmittgen, 2001). For analysis of *Fractalkine* and *Cx3cr1* mRNA expression in the developing cortex, data was normalized to the E12.5 cortical sample. For shCX3CR1 validation experiments in HEK293

cells, data was compared to cells transfected with the mouse CX3CR1 expression plasmid and scrambled shRNA. All primers were validated and qRT-PCR assays were performed in accordance with MIQE guidelines (Bustin et al., 2009). The following primers were used for qRT-PCR analysis: *Fkn* 5′- ACGAAATGCGAAATCATGTGC-3′ (forward) and 5′-CTGTGTCGTCTCCAGGACAA-3′ (reverse); *Cx3cr1* 5′-CGGCCATCTTAGTGGCGTC-3′ (forward) and 5′-GGATGTTGACTTCCGAGTTGC-3′ (reverse); *mouse Gapdh* 5′-GGGTGT GAACCACGAGAAATA-3′ (forward) and 5′-CTGTGGTCATGAGCCCTTC-3′ (reverse) and *human Gapdh* 5′-TGGTGCTGAGTATG TCGTGGAGT-3′ (forward) and 5′-AGTCTTCTGAGTGGCAGTGATGG-3′ (reverse).

Computational analysis

Microarray data were analyzed as previously described (Yuzwa et al., 2016). Raw probe intensity values were background corrected, normalized with quantile normalization, transformed into the $\log_2$ scale, and summarized into probesets using the Robust Multichip Analysis (RMA) algorithm using the Oligo bioconductor package in R (Carvalho and Irizarry, 2010). Genes encoding ligands were extracted from the microarray data (GEO: GSE95696) using Python (version 2.7.6) code and a curated database of secreted factors (Qiao et al., 2014; Yuzwa et al., 2016) with a cut-off of 40% of the highest log2 expression values. This analysis yielded 90 potential secreted ligands expressed by the MGE neurons (Table S1). Genes encoding receptors were extracted using a similar approach to analyze previously-published cortical precursor cell microarray data (GEO: GSE84482) (Yuzwa et al., 2016). The interneuron-specific ligand and cortical precursor-specific receptor databases were then used to build the interneuron-cortical precursor communication model using Cytoscape (version 3.1.0) as described (Johnston et al., 2016;Yuzwa et al., 2016).

Enzyme-linked immunosorbant assay (ELISA)

Commercially available ELISA kits (Ray Biotech) were used to measure the concentrations of Gas6, VEGFA and fractalkine in medium conditioned by MGE interneurons, prepared as described above. ELISA measurements were performed with three independent preparations of MGE interneuron conditioned medium.

QUANTIFICATION AND STATISTICAL ANALYSIS

Quantification of immunostained cell cultures and brain sections was performed as described in (Gallagher et al., 2015; Yuzwa et al., 2016). Briefly, cell cultures were analyzed with a Zeiss Axioplan2, Zeiss Axio Imager M2 or Olympus IX81 fluorescence microscope equipped with Okogawa CSU X1 spinning disk confocal scan head. Digital image acquisition was performed with Axiocam (Zeiss), ZEN (Zeiss) or Volocity (Perkin Elmer) software using a Hamamatsu camera (Hamamatsu). In all culture experiments except when cells were transfected with plasmids, 3-5 random fields of view were captured with 20X or 40X objective. For cell identity analysis, at least 300 cells from different fields were counted per condition and results are from at least three independent experiments. For clonal experiments, over 100 clones were analyzed per condition per experiment. In our culture conditions, less than 1% of cells are transfected allowing for clonal analysis (Gallagher et al., 2015; Yuzwa et al., 2016). A clone was defined as a cluster of eGFP-positive cells in close proximity to each other, which were clearly separated from other eGFP-positive clusters (Gallagher et al., 2015; Yuzwa et al., 2016). For knockdown and rescue experiments, at least 1000 GFP-positive cells were analyzed per condition per experiment. Results are presented as % marker-positive cells relative to total counted GFP-positive cells from three independent experiments. For BrdU quantification in vitro, results are presented as the proportion of BrdU-positive, marker-positive cells relative to total marker-positive cells. For in utero electroporation, 3-4 anatomically matched sections per brain from at least three embryos or pups from different mothers were imaged with a 20X objective on a Zeiss Axio Imager M2 system with an X-Cite 120 LED light source and a C11440 Hamamatsu camera. A cortical area from SVZ to meninges and containing GFP-positive cells was imaged and the same size column spanning SVZ to meninges was counted for marker-positive and GFP-positive cells. The results are presented as the percentage of marker-positive cells relative to total GFP-positive cells. For immunocytochemical analysis of genetic ablation or CX3CR1 knockout experiments, 4 anatomically matched sections per brain from at least three embryos or pups from different mothers were imaged and analyzed as described for in utero electroporation. Results are presented as mean marker-positive cells per section. For BrdU quantification in vivo, results are presented as the proportion of marker-positive cells relative to total BrdU-positive cells. For FISH experiments, sections were imaged with an Olympus IX81 fluorescence microscope equipped with a Hamamatsu C9100-13 back-thinned EM-CCD camera and Okogawa CSU X1 spinning disk confocal scan head. Z stacks of confocal images were taken with optical slice thickness 0.2 μm and stacked images are shown. For quantification of *Fkn*-positive cells, cells containing 3 or more *Fkn* FISH dots were counted in 4 consecutive sections in the SVZ area from anatomically matched brain sections. Images were processed using Axiocam (Zeiss), ZEN (Zeiss) or Volocity (Perkin Elmer) software. At E15.5, the VZ was defined by Pax6 staining and IZ and CP were defined by Hoechst staining. At E18.5 and P0, the cortical SVZ was defined by Sox2 staining. At P0 apical cortex was defined by Olig2 staining. At P15, the corpus callosum was defined by CC1 and Olig2 staining.

Sample sizes (n) indicated in the figure legends 1, 2, 4, 5, 8A-F correspond to the number of biological replicates analyzed. Sample sizes (n) indicated in the figure legends 3, 6A, 6L, 7, 8H-T correspond to the number of brains from at least two independent litters analyzed. All statistical parameters are presented as means ± SEM (Standard Error of the Mean). All in vivo datasets passed the analysis for Gaussian distribution using Shapiro-Wilk normality test and the statistical significance was assessed as described below (based on at least 4 sections per brain, 3-5 brains per experiment). For in vitro experiments, relatively small sample size (n = 3-4) did not allow us to analyze the datasets for Gaussian distribution. The predominant statistical analysis method carried out for

in vitro datasets was the Student's t test. This test is well suited to handle cases where sample size is relatively low and the assumption of normality of the data cannot be easily assessed. Additionally, this statistical approach is applied broadly across the field. For all datasets, the statistical significance was assessed as follows: 1) for two group comparisons, two-tailed unpaired Student's t tests were used to assess statistical significance between means, where a p value < 0.05 was considered significant; 2) for three or more group comparisons, one-way ANOVA followed by Newman-Keuls post hoc test (figure legends 3, 4H-K, 6L, 7B-H, 7R-S, 8C-F, 8T), Dunnett's post hoc test (figure legends 4C-F) or two-way ANOVA followed by Bonferroni post hoc test (figure legend 2K) were used to assess statistical significance between means, where a p value < 0.05 was considered significant. In all cases, Prism (version 5.0a) was used. Number of experiments and statistical information are stated in the corresponding figure legends. In figures, asterisks denote statistical significance marked by *, $p < 0.05$; **, $p < 0.01$; ***, $p < 0.001$. In all figures, all samples or mice were used without exclusion.

DATA AND SOFTWARE AVAILABILITY

The MGE interneuron expression data have been deposited in the GEO database under ID code GEO: GSE95696.